

8f. Neutrons

MURREY D. GOLDBERG

Brookhaven National Laboratory

JOHN A. HARVEY

Oak Ridge National Laboratory

Neutrons have been extensively used as probes to investigate the properties of nuclei ever since the discovery of the neutron in 1932. Its lack of charge gives it an advantage over charged particles in many experimental areas, although the inability to define its energy to the same precision as that of charged particles counters this advantage in other areas of nuclear structure studies. Neutrons are available in copious supply from many sources throughout an energy range extending from below 10^{-4} eV to above 100 MeV. An enormous number of data have been accumulated, covering a wide variety of nuclear interactions for all nuclides of the periodic table.

No attempt will be made to even summarize the data here. For a detailed compilation of neutron cross-section experimental data, the reader is referred to the many volumes of the report BNL-325 (1958, 1960, 1964-1966) for cross-section data at thermal energies, for parameters of compound-nucleus resonances due to neutron interactions, and for energy-dependent cross-section data through the entire energy range; and to the report BNL-400 (1970) for angular distribution data. (A complete bibliography of these reports is given in Sec. 8f-10.)

For the techniques involved in neutron physics measurements, the reader is referred to the two-volume work "Fast Neutron Physics," edited by J. B. Marion and J. L. Fowler and published by Interscience Publishers, Inc., New York (part I in 1960; part II in 1963); and to "Experimental Neutron Resonance Spectroscopy" edited by J. A. Harvey and published by Academic Press, Inc., New York, 1970.

This section contains selected topics which seem appropriate. A noticeable omission is a table of thermal neutron cross sections. Such a listing can be found in the Table of Isotopes by D. T. Goldman (Sec. 8b), and is not duplicated here.

8f-1. Neutron Properties. Where needed to obtain quantities for this table, the values of physical constants used were taken from B. N. Taylor, W. H. Parker, and D. N. Langenberg, *Rev. Mod. Phys.* **41**, 375 (1969):

Spin, $\hbar/2$

Statistics, Fermi-Dirac

Radioactive decay, half life = 11.0 ± 0.3 min; beta-decay energy = 782.45 ± 0.07 keV

Magnetic moment $\mu_n = -1.913159 \pm 0.000047$ nuclear magnetons

Neutron mass, $1.00866520 \pm 0.00000010$ mass units [unified scale, $C^{12} = 12$],
 $(1.674920 \pm 0.000011) \times 10^{-24}$ g, 939.5527 ± 0.0052 MeV

Compton wavelength:

$$\lambda_c = h/m_nc = (1.3196217 \pm 0.0000090) \times 10^{-13} \text{ cm}$$

$$\lambda_c = \lambda_c/2\pi = (2.100243 \pm 0.000014) \times 10^{-14} \text{ cm}$$

Nonrelativistic conversion formulas [E (eV) as function of T (K), v (m/sec), and λ (cm)]:

$$E = kT = 8.6171 \times 10^{-5}T$$

$$E = m_nv^2/2 = 5.22695 \times 10^{-9}v^2$$

$$E = h^2/2m_n\lambda^2 = 8.18015 \times 10^{-18}/\lambda^2$$

For a neutron velocity of 2,200 m/sec:

$$E = 0.0252984 \text{ eV}$$

$$T = 293.58 \text{ K}$$

$$\lambda = 1.79818 \times 10^{-8} \text{ cm}$$

Figures 8f-1 to 8f-3 provide graphs from which reasonably accurate values of the relationships between energy-dependent properties can be read. The formula for

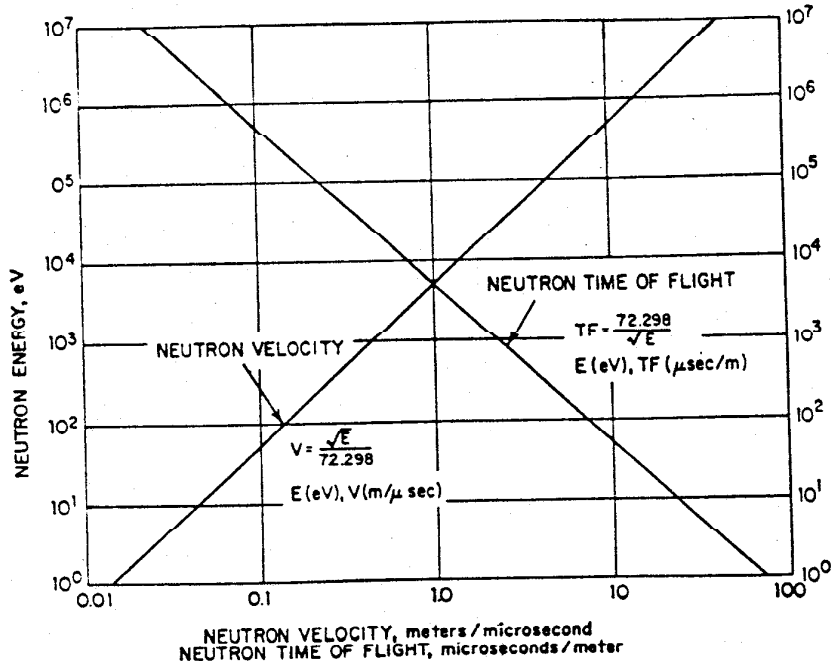


FIG. 8f-1. Variation of neutron velocity and neutron time of flight with energy for the neutron energy range 1 eV to 10 MeV.

NUCLEAR PHYSICS

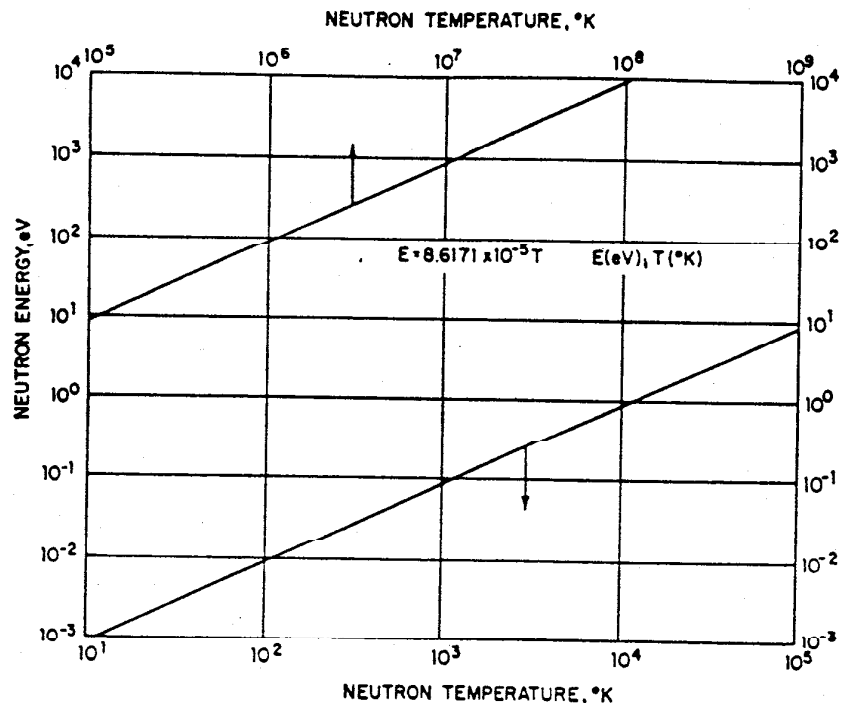


FIG. 8f-2. Variation of neutron temperature with energy for the neutron energy range 0.001 eV to 10 keV.

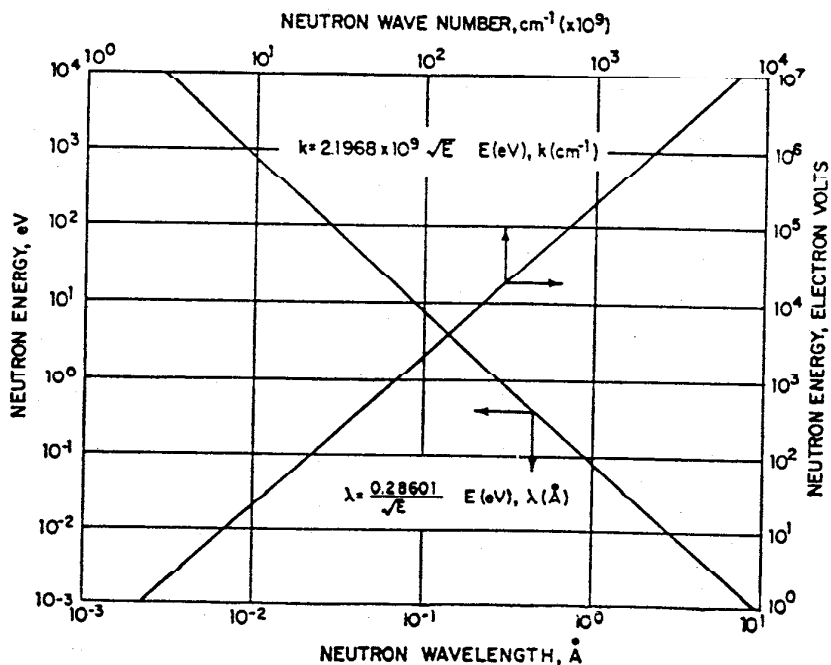


FIG. 8f-3. Variation of neutron wavelength with energy for the neutron energy range 0.001 eV to 10 keV and the variation of the neutron wave number with energy for the neutron energy range 1 eV to 10 MeV.

each relationship is given on the curve so that more accurate values can be obtained quickly when needed or can be calculated for values at energies outside the range included in the graph.

8f-2. Neutron Separation Energies. The compound nucleus ($A + 1$) formed by the addition of a neutron to a target nuclide A at rest has an excitation energy equal to the neutron's separation energy B_n of the compound nucleus plus the neutron's kinetic energy E_n minus the compound nucleus' recoil energy [$\sim E_n/(A + 1)$]. The energy of the gamma radiation to the ground state of the residual nucleus will equal the excitation energy of the compound nucleus plus its kinetic energy minus the kinetic energy of the residual nucleus. For example, the energy of the ground-state gamma ray from the capture of *thermal* neutrons by ^{14}N will be the neutron separation energy of ^{15}N ($10,834.0 \pm 0.8$ keV) minus the recoil energy of ^{15}N [$\sim 0.537(E_\gamma^2/\text{MeV})/(A + 1)$] keV = 4.2 keV} which equals 10,829.8 keV. For a photoneutron reaction, the energy of the gamma ray will have to exceed the neutron separation energy of the target nuclide by the recoil energy of the compound nucleus. For example, for the photo-disintegration of the deuteron, the gamma ray's energy must exceed the neutron separation of deuterium ($2,224.55 \pm 0.07$ keV) by the recoil energy 1.32 keV.

Neutron separation energies with standard deviations are listed in Table 8f-1 for the stable nuclides, for radioactive nuclides with half lives $> 1,000$ years, for shorter-lived radioactive nuclides which have been produced in milligrams or larger quantities, and for these nuclides plus a neutron. The values for the neutron separation energies come principally from least-squares adjustments of experimental data by J. H. E. Mattauch, W. Thiele, and A. H. Wapstra, *Nuclear Physics* 67, 32 (1965); by A. H. Wapstra, C. Kurzeck, and A. Anisimoff, *Proceedings of the Third International Conference on Atomic Masses*, August 28-September 1, 1967, edited by R. C. Barber, University of Manitoba Press; and from vols. I and II, sec. B of the *Nuclear Data Sheets*, Academic Press, Inc. Recent accurate values obtained from the (n, γ) reaction were taken from a Compendium of Thermal Neutron Capture γ -ray Measurements, part I, $Z \leq 46$, *Nuclear Data A3* (4-6), 367 (1967); part II, $Z = 47$ to $Z = 67$ (Ag to Ho), *Nuclear Data Tables A5* (1-2), 1 (1968); part III, $Z = 68$ to $Z = 94$ (Er to Pu), *Nuclear Data Tables A5* (4-5), 243 (1969); and from recent accurate unpublished (n, γ) data. For nuclides where no error is assigned, the neutron separation energies were estimated from nuclear systematics.

8f-3. Coherent Scattering Amplitudes. Since the wavelengths of thermal neutrons are of the order of one angstrom, their scattering interactions with matter exhibit such well-known optical phenomena as diffraction and refraction. A scattering interaction can be characterized by an *amplitude*, which represents the distance that the neutron wave is shifted by the scattering nucleus.

For a nucleus of nonzero spin, there will be two amplitudes, a_+ and a_- , corresponding to the two possible spin states of the compound nucleus, $I \pm \frac{1}{2}$, formed by the combination of a neutron (spin $\frac{1}{2}$) with a target nucleus (spin I). The compound states are not equally probable but are weighted in the ratio $(I + 1)$ to I . Hence, the *coherent amplitude*, which is the weighted mean of the two amplitudes, is given by

$$a_{\text{coh}} = \frac{I + 1}{2I + 1} a_+ + \frac{I}{2I + 1} a_-$$

The *coherent cross section*, neglecting interference with other nuclei, will then be given by $4\pi a_{\text{coh}}^2$. The coherent amplitude for an element with two or more isotopes can be obtained from

$$a_{\text{coh}} = \sum f_i a_i$$

NUCLEAR PHYSICS

TABLE 8f-1. TABLE OF NEUTRON SEPARATION ENERGIES

Atomic no. <i>Z</i>	Element	Mass no. <i>A</i> = <i>N</i> + <i>Z</i>	Number of neutrons <i>N</i>	Separation energy <i>B_n</i> , keV	Atomic no. <i>Z</i>	Element	Mass no. <i>A</i> = <i>N</i> + <i>Z</i>	Number of neutrons <i>N</i>	Separation energy <i>B_n</i> , keV
1	H	2	1	2,224.55 ± 0.07	20	Ca	48	28	9,940 ± 11
2	He	3	2	6,257.4 ± 0.1	49		49	29	5,144 ± 6
3	Li	4	2	20,578.0 ± 0.4	21	Sc	45	24	11,319 ± 6
		5	3	- 958 ± 19			46	25	8,766.6 ± 3.9
		6	3	5,662 ± 37	22	Ti	46	24	13,192 ± 5
4	Be	7	4	7,252.5 ± 1.3			47	25	8,875.4 ± 2.5
		8	5	2,032.5 ± 1.0			48	26	11,628.0 ± 2.7
5	B	9	5	1,665.1 ± 0.6			49	27	8,146.0 ± 2.2
		10	6	6,811.8 ± 0.4			50	28	10,944.4 ± 3.5
		10	5	8,437.9 ± 1.4			51	29	6,379 ± 5
6	C	11	6	11,455.9 ± 0.5	23	V	50	27	9,337 ± 5
		12	7	3,368.9 ± 1.4			51	28	11,054.6 ± 3.9
		12	6	13,719.8 ± 1.1			52	29	7,308.8 ± 4.4
7	N	13	7	4,946.5 ± 0.2	24	Cr	50	26	12,930 ± 11
		14	8	8,176.2 ± 0.9			51	27	9,261 ± 3
		15	9	1,218.0 ± 0.8			52	28	12,034.9 ± 3.9
8	O	14	7	10,552.9 ± 1.1			53	29	7,941.4 ± 3.1
		15	8	10,834.0 ± 0.8			54	30	9,719 ± 2
		16	9	2,486.7 ± 3.5			55	31	6,254 ± 6
9	F	16	8	15,667.9 ± 1.2	25	Mn	55	30	10,225 ± 6
		17	9	4,142.5 ± 0.9			56	31	7,270.4 ± 3.1
10	Ne	18	10	8,046.2 ± 0.9	26	Fe	54	28	13,396 ± 16
		19	11	3,956.3 ± 2.9			55	29	9,299.5 ± 3.9
		19	10	10,429.9 ± 1.0			56	30	11,203.3 ± 4.6
11	Na	20	11	6,602 ± 1			57	31	7,646.5 ± 1.0
		20	10	16,865.0 ± 1.6			58	32	10,043.1 ± 1.0
12	Mg	21	11	6,759.8 ± 1.5			59	33	6,586.3 ± 4.1
		22	12	10,366.5 ± 1.5			60	34	8,864 ± 30
		23	13	5,194.9 ± 3.3			61	35	5,730 ± 50
11	Na	23	12	12,417.6 ± 3.2	27	Co	59	32	10,461.1 ± 4.9
		24	13	6,959.3 ± 0.4			60	33	7,491.6 ± 1.9
12	Mg	24	12	16,532.4 ± 3.2	28	Ni	58	30	12,195 ± 16

NEUTRONS

TABLE 8f-1. TABLE OF NEUTRON SEPARATION ENERGIES (*Continued*)

Atomic no. <i>Z</i>	Element	Mass no. <i>A = N + Z</i>	Number of neutrons <i>N</i>	Separation energy <i>B_n</i> , keV		Atomic no. <i>Z</i>	Element	Mass no. <i>A = N + Z</i>	Number of neutrons <i>N</i>	Separation energy <i>B_n</i> , keV
				46	46					
34	Se	60	46	9,902.8	± 4.9	Pd	106	60	9,544	± 4
		81	47	6,715	± 6					
		82	48	9,262	± 9					
35	Br	83	49	5,970	± 50	108	61	61	6,532	± 7
		79	44	10,698	± 6					
		80	45	7,876.0	± 4.4					
36	Kr	81	46	10,164	± 6	Ag	107	60	9,531	± 9
		82	47	7,601	± 8					
		78	42	12,010	± 50					
37	Rb	79	43	8,340	± 8	Cd	108	61	7,267	± 1
		80	44	11,520	± 9					
		81	45	7,850	± 100					
38	Sr	82	46	10,980	± 100	In	109	62	9,182	± 9
		83	47	7,467	± 6					
		84	48	10,519	± 5					
39	Y	85	49	7,122	± 6	Sn	110	63	6,810	± 1
		86	50	9,848	± 7					
		87	51	5,511	± 8					
40	Zr	85	48	10,475	± 6	114	62	58	10,870	± 1
		86	49	8,637	± 9					
		87	50	9,940	± 7					
38	Sr	88	51	6,130	± 90	49	111	63	7,929	± 7
		84	46	11,580	± 1					
		85	47	8,482	± 31					
39	Y	86	48	11,522	± 31	50	112	64	10,334	± 7
		87	49	8,437	± 5					
		88	50	11,113	± 1					
40	Zr	89	51	6,363	± 8	113	65	6,738.2	± 3.8	
		90	50	11,477	± 8					
		91	51	6,857	± 2					
39	Y	90	51	11,997	± 6	114	66	6,143	± 9	
		90	50	7,194	± 5					
		91	51	7,194	± 5					
40	Zr	90	51	6,857	± 2	115	68	8,694	± 9	
		90	50	11,997	± 6					
		91	51	7,194	± 5					
39	Y	91	51	7,194	± 5	116	67	6,725	± 23	
		91	50	11,477	± 8					
		92	51	6,857	± 2					
40	Zr	91	51	11,997	± 6	117	66	7,537	± 9	
		91	50	7,194	± 5					
		92	51	7,194	± 5					
39	Y	92	51	6,857	± 2	118	67	10,320	± 16	
		92	50	11,477	± 8					
		93	51	6,857	± 2					
40	Zr	92	51	11,997	± 6	119	66	9,563	± 7	
		92	50	7,194	± 5					
		93	51	7,194	± 5					
39	Y	93	51	6,857	± 2	120	67	6,941	± 5	
		93	50	11,477	± 8					
		94	51	6,857	± 2					

NEUTRONS

TABLE 8f-1. TABLE OF NEUTRON SEPARATION ENERGIES (Continued)

Atomic no. Z	Element	Mass no. $A = N + Z$	Number of neutrons N	Separation energy B_n , keV	Atomic no. Z	Element	Mass no. $A = N + Z$	Number of neutrons N	Separation energy B_n , keV
54	Xe	135	81	6,530 ± 100	66	Dy	160	94	8,590 ± 30
		136	82	7,380 ± 100			161	95	6,448 ± 12
		137	83	4,460 ± 100			162	96	8,193 ± 3
55	Cs	133	78	9,038 ± 27			163	97	6,270 ± 3
		134	79	6,705 ± 15			164	98	7,654 ± 3
		135	80	9,050 ± 110			165	99	5,715 ± 2
56	Ba	136	81	6,610 ± 70	67	Ho	165	98	8,043 ± 36
		130	74	10,260			166	99	6,243 ± 3
		131	75	7,695 ± 12			167	100	7,290 ± 100
		132	76	9,360 ± 280	68	Er	162	94	9,200
		133	77	7,257 ± 42			163	95	6,840 ± 90
		134	78	9,252 ± 16			164	96	8,795 ± 42
		135	79	6,974 ± 3			165	97	6,645 ± 40
		136	80	9,106.4 ± 0.8			166	98	8,549 ± 33
		137	81	6,904 ± 4			167	99	6,436.2 ± 0.5
		138	82	8,611.1 ± 0.8			168	100	7,771.2 ± 0.5
		139	83	4,723.4 ± 0.7			169	101	5,997 ± 12
57	La	138	81	7,260			170	102	7,190 ± 70
		139	82	8,792 ± 20			171	103	5,676 ± 10
		140	83	5,161.0 ± 1.0	69	Tm	169	100	8,055 ± 35
58	Ce	136	78	9,990			170	101	6,595 ± 2.5
		137	79	7,840	70	Yb	168	98	8,980 ± 0.5
		138	80	9,470			169	99	6,867.2 ± 0.5
		139	81	7,598 ± 26			170	100	8,550 ± 35
		140	82	9,039 ± 48			171	101	6,616 ± 3
		141	83	5,428.6 ± 0.6			172	102	8,023 ± 3
		142	84	7,159 ± 8			173	103	6,365 ± 3
		143	85	5,182 ± 10			174	104	7,465 ± 3
59	Pr	141	82	9,386 ± 18			175	105	5,819 ± 3
		142	83	5,843.6 ± 1.2			176	106	6,640 ± 80
60	Nd	142	82	9,899 ± 9			177	107	5,565 ± 16
		143	83	6,123 ± 2	71	Lu	175	104	7,801 ± 42
		144	84	7,87.2 ± 1.8			176	105	6,293.2 ± 1.2
		145	85	5,760.4 ± 1.9			177	106	6,890 ± 2

NEUTRONS

NUCLEAR PHYSICS

TABLE 8f-1. TABLE OF NEUTRON SEPARATION ENERGIES (*Continued*)

TABLE II. TABLE OF NEUTRON SEPARATION ENERGIES (Continued)

Atomic no. <i>Z</i>	Element	Mass no. <i>A</i> = <i>N</i> + <i>Z</i>	Separation energy <i>R_n</i> , keV		Number of neutrons <i>N</i>	Atomic no. <i>Z</i>	Element	Mass no. <i>A</i> = <i>N</i> + <i>Z</i>	Number of neutrons <i>N</i>	Separation energy <i>B_n</i> , keV											
			193	194	195	196	197	198	199	200	201	202	203	204	205	206	207	208	209	226	227
78	Pt	115	6,288	± 48	116	8,384	± 20	117	6,126	± 13	118	7,920	9 ± 1.5	119	5,854	± 14	120	7,561	19	91	Pa
79	Au	116	6,288	± 48	117	8,384	± 20	118	6,126	± 13	119	7,920	9 ± 1.5	120	5,854	± 14	121	5,570	19	92	U
80	Hg	116	6,288	± 48	117	8,384	± 20	118	6,126	± 13	119	7,920	9 ± 1.5	120	5,854	± 14	121	5,570	19	93	Np
81	Tl	117	6,288	± 48	118	8,384	± 20	119	6,126	± 13	120	7,920	9 ± 1.5	121	5,854	± 14	122	5,570	19	94	Pu
82	Pb	118	6,288	± 48	119	8,384	± 20	120	6,126	± 13	121	7,920	9 ± 1.5	122	5,854	± 14	123	5,570	19	95	Am
83	Bi	119	6,288	± 48	120	8,384	± 20	121	6,126	± 13	122	7,920	9 ± 1.5	123	5,854	± 14	124	5,570	19	96	Cm
88	Ra	120	6,288	± 48	121	8,384	± 20	122	6,126	± 13	123	7,920	9 ± 1.5	124	5,854	± 14	125	5,570	19	97	U

where the f_i are the abundances ($\sum f_i = 1$) of the individual isotopes with coherent amplitudes a_i . The *index of refraction* for a noncapturing medium can be calculated from the coherent scattering amplitude as

$$n^2 = 1 - \frac{\lambda^2 N a_{coh}}{\pi}$$

where λ is the neutron wavelength, and N is the number of nuclei per cm^3 .

Table 8f-2 lists the coherent scattering amplitudes for those elements, or particular isotopes, for which experimental values have been determined. The amplitude values are given in femtometers ($\equiv 10^{-13} \text{ cm}$) and are preceded by a positive or negative sign. The standard convention adopted here is that positive amplitude represents hard-sphere scattering, i.e., a phase shift of 180 deg. For two values the sign is omitted, since no explicit experimental assignment has been made, but both cases are probably positive.

8f-4. Recommended 2,200-m/sec Cross Sections for Fissile Isotopes. In Table 8f-3, which is taken from G. C. Hanna, C. H. Westcott, H. D. Lemmel, B. R. Leonard, Jr., J. S. Story, and P. M. Attree, *Atomic Energy Rev.* 7, (4) 3 (1969), IAEA, Vienna, the results of a careful study of relevant experimental measurements are presented. A least-squares fitting procedure was used, and both direct and indirect measurements of the quantities listed were considered.

The quantities appearing in the table have the following meanings:

- σ_a Absorption cross section: $\sigma(n, \gamma) + \sigma(n, f) = \sigma_{tot} - \sigma_{scat}$
- σ_f Fission cross section: $\sigma(n, f)$
- σ_γ Radiative capture cross section: $\sigma(n, \gamma)$
- α Ratio: $\sigma(n, \gamma)/\sigma(n, f)$
- η Number of neutrons produced per absorption event: prompt + delayed
- $\bar{\nu}_T$ Number of neutrons produced per fission event: prompt + delayed

The ν value for Cf²⁵², which is the standard used in the fissile ν measurements, was evaluated to be 3.765 ± 0.012 .

8f-5. s-wave Neutron Strength Functions, Observed Resonance Spacings, and Average Radiation Widths. Neutron cross sections of most nuclides exhibit individual resonances in the energy region from 0.1 eV to 100 keV. These resonances correspond to excited states of the compound nucleus at an excitation energy just above the neutron separation energy. The resonances can be described by the following parameters:

- E_0 Resonance energy
- Γ Total width
- Γ_n Neutron width
- Γ_γ Radiation width
- Γ_F Fission width
- l Angular momentum of the neutron, s, p, d , etc.
- J Spin of the compound nucleus

Since the parameters of over 10,000 resonances have now been measured, it is not possible to present a complete listing of these parameters in this section. The detailed parameters may be found in the many volumes of the report BNL-325 (1958, 1960, 1964-1966). However, for many purposes the average of the parameters for each nuclide are sufficient. Some of these averages for s-wave interactions which are predominant in the energy region $\lesssim 10 \text{ keV}$ are listed in Table 8f-4.

The s-wave neutron strength function for a nuclide is defined as Γ_n^o/D . Γ_n^o is the average of the reduced neutron widths Γ_n^o of s-wave resonances of the same spin and parity, where Γ_n^o is equal to $\Gamma_n/\sqrt{E_0}$ (in eV). D is the average level spacing for resonances of the same spin and parity. s-wave strength functions can be determined from the parameters of resolved resonances or from the energy dependence of the

NUCLEAR PHYSICS

TABLE 8f-2. COHERENT SCATTERING AMPLITUDES

Atomic no. <i>Z</i>	Element	Mass no. <i>A</i> = <i>N</i> + <i>Z</i>	Coherent amplitude <i>a</i> _{coh.} , fm	Atomic no. <i>Z</i>	Element	Mass no. <i>A</i> = <i>N</i> + <i>Z</i>	Coherent amplitude <i>a</i> _{coh.} , fm
1	H	1	-3.719 ± 0.002	47	K	107	+6.1 ± 0.4
		2	+6.21 ± 0.04			109	+8.3 ± 0.5
2	He	3	+4.7 ± 0.3			...	+4.3 ± 0.4
3	Li	...	+3.0 ± 0.5	48	Cd	...	+3.32 ± 0.20
		6	-1.94 ± 0.05	49	In	...	+3.8 ± 0.1
		7	+1.8 ± 0.05	50	Sn	...	+6.1 ± 0.4
4	Be	7	-2.1			116	+5.8 ± 0.4
5	B	...	+7.74 ± 0.07			117	+6.4 ± 0.25
		10	+5.40 ± 0.04			118	+5.8 ± 0.1
		11	+6.53 ± 0.35			119	+6.0 ± 0.25
6	C	...	+6.1 ± 0.1			120	+6.4 ± 0.1
		13	+6.656 ± 0.004			122	+5.5 ± 0.3
7	N	...	+6.0 ± 0.8			124	+5.9 ± 0.2
8	O	...	+9.14 ± 0.10	51	Sb	...	+5.4 ± 0.1
9	F	...	+5.80 ± 0.05	52	Te	...	+5.6 ± 0.4
10	Ne	...	+5.6 ± 0.1			120	+5.3 ± 0.1
11	Na	...	+4.60 ± 0.05			123	+5.8 ± 0.7
12	Mg	...	+3.5 ± 0.1			124	+5.5 ± 0.5
13	Al	...	+5.2 ± 0.1			125	+5.6 ± 0.6
14	Si	...	+3.5 ± 0.3			130	5.7 ± 0.6
15	P	...	+4.1646 ± 0.0022	53	I	...	+5.2 ± 0.3
16	S	...	+5.1 ± 0.1	54	Xe	...	+4.62 ± 0.09
17	Cl	...	+3.1 ± 0.2	55	Cs	...	+4.9 ± 0.3
18	Ar	...	+9.9 ± 0.6	56	Ba	...	+5.3 ± 0.3
19	K	...	+1.89 ± 0.02	57	La	...	+8.3 ± 0.6
20	Ca	...	+3.70 ± 0.04	58	Ce	...	+4.84 ± 0.06
		40	+4.88 ± 0.07			140	+4.7 ± 0.2
		44	+4.9 ± 0.2			142	+4.5 ± 0.4
		44	+1.3 ± 0.1	59	Pr	...	+4.4 ± 0.4
21	Sc	...	+11.3 ± 1.0	60	Nd	...	+7.2 ± 0.6
22	Ti	...	-3.5 ± 0.1			142	+7.7 ± 0.6
		46	+4.3 ± 0.2			144	+2.8 ± 0.6
		47	+3.3 ± 0.2			146	+8.7 ± 0.4

NEUTRONS

8-231

23	V	48	-5.8	+0.3	61	152	-5	+2
24	Cr	49	+0.8	+0.2	62	154	+8	+2
		50	+5.5	+0.3	63	Eu	+6.3	+0.3
		...	-0.5	+0.1	64	Gd	+15	+2
25	Mn	52	+3.52	+0.06	65	Tb	+7.56	+0.20
26	Fe	54	+4.9	-3.7	66	Dy	+16.9	+0.4
		56	+4.2	+0.2			+6.7	+0.4
		57	+10.1	+0.2			+10.3	+0.4
27	Co	58	+2.3	+0.1			-1.4	+0.5
28	Ni	60	+2.5	+0.3			162	+0.5
		61	+10.3	+0.2	67	Ho	+5.0	+0.4
		62	+14.4	+0.2	68	Er	+49.4	+0.5
		64	+3.0	+0.3	69	Tm	+8.5	+0.2
		65	+7.60	+0.06	70	Yb	+7.9	+0.4
		66	-8.7	+0.4	71	Lu	+7.20	+0.06
		67	-0.38	+0.07	72	Hf	+12.90	+0.07
		68	+7.7	+0.3	73	Ta	+7.3	+0.2
		69	+6.72	+0.15	74	W	+7.77	+0.14
		70	+11.1	+0.2	75	Re	+7.0	+0.5
		71	+5.7	+0.1	76	Os	+4.66	+0.09
29	Cu	73	+8.4	+0.5			+9.2	+0.09
		74	+6.4	+0.1			+10.7	+0.09
		75	+7.2	+0.1			+11.0	+0.09
		76	+8.4	+0.5			+11.4	+0.09
30	Zn	77	+6.4	+0.1			+12.68	+0.02
	Ga	78	+7.79	+0.14			+8.9	+0.9
31	Ge	79	+6.7	+0.5			+9.34	+0.02
32	As	80	7.44	+0.15			+8.5239	+0.0014
33	Se	81	+8.5	+0.1			+9.8	+0.1
34	Br	82	+8.3	+0.1			+8.4	+0.2
35	Kr	83	+6.83	+0.07			+9.8	+0.6
36	Rb	84	+7.88	+0.05			+10.57	+0.06
37		85	+7.0	+0.2			+7.5	+0.3
38	Sr	86	+6.9	+0.2			+3.8	+3.8
39	Y	87	+6.7	+0.2				
40	Zr	88	+6.8	+0.3				
41	Nb	89	+7.3	+0.7				
42	Mo	90	+7.0	+0.2				
43	Tc	91	+6.9	+0.2				
44	Ru	92	+6.8	+0.3				
45	Rh	93	+6.8	+0.3				
46	Pd	94	+6.0	+0.7				
		95	+5.9	+0.9				

NUCLEAR PHYSICS

TABLE 8f-3. RECOMMENDED 2,200-M/SEC CROSS SECTIONS FOR FISSION ISOTOPES

Parameter	U^{233}	U^{235}	Pu^{239}	Pu^{241}
σ_a	577.6 ± 1.8	678.5 ± 1.9	1012.9 ± 4.1	1375.4 ± 8.6
σ_f	530.6 ± 1.9	580.2 ± 1.8	741.6 ± 3.1	1007.3 ± 7.2
σ_γ	47.0 ± 0.9	98.3 ± 1.1	271.3 ± 2.6	368.1 ± 7.8
α	0.0885 ± 0.0018	0.1694 ± 0.0021	0.3659 ± 0.0039	0.3654 ± 0.0090
η	2.2844 ± 0.0063	2.0719 ± 0.0060	2.1085 ± 0.0066	2.149 ± 0.014
ν_T	2.4866 ± 0.0069	2.4229 ± 0.0066	2.8799 ± 0.0090	2.934 ± 0.012

total cross section averaged over many resonances. The values with standard deviations listed in Table 8f-4 were taken principally from a compilation by K. K. Seth, *Nuclear Data A2*, 299 (Sept. 1966). Standard deviations are given for values where the errors are less than 50 percent of the value. A few spin- $\frac{3}{2}$ target nuclides have s-wave strength functions which are different for the two compound nucleus spin states 1 and 2. For these nuclides the s-wave strength function for the resonances with $J = 2$ is approximately twice that for $J = 1$ resonances.

The values for the observed resonance spacings with standard deviations for s-wave neutrons D_{obs} listed in Table 8f-4 were taken principally from a summary by J. E. Lynn, "The Theory of Neutron Resonance Reactions," Clarendon Press, Oxford, 1968. For zero-spin target nuclides, the average level spacing D for resonances with $J = \frac{1}{2}$ is equal to D_{obs} . For nonzero-spin target nuclides, D for the two spin states is greater than D_{obs} and may be computed from the formula

$$D_J = 2D_{obs} \frac{2I+1}{2J+1}$$

where I = spin of target nucleus

J = spin of compound nucleus

$J = I \pm \frac{1}{2}$ for s-wave resonances

For example, for $I = \frac{1}{2}$, $D_{J=0} = 4D_{obs}$ and $D_{J=1} = \frac{4}{3}D_{obs}$. Several of the values listed as lower limits were determined from the energy of only the lowest resonance.

The values of the average radiation widths with standard deviations for s-wave neutrons Γ_γ listed in Table 8f-4 were determined principally from the resonance data tabulated in BNL-325 (1958, 1960, 1964-1966). The standard deviation includes both the experimental errors in the measurements of the radiation widths of the individual resonances and the standard deviation arising from the width of the distribution of Γ_γ . For heavy nuclides the width of the distribution is ~ 10 percent corresponding to a chi-squared distribution with 200 degrees of freedom, while for light nuclides the width is ~ 30 percent which corresponds to ~ 22 degrees of freedom.

Values denoted with an asterisk are based on data for only one or two resonances and sometimes are computed from thermal capture cross sections or resonance capture integrals. These values with an asterisk may not include the standard deviation arising from a poor sampling from the distribution of Γ_γ . Hence, the correct Γ_γ for these nuclides might be different from the value listed by ~ 10 to ~ 30 percent. A few nonzero-spin target nuclides have average radiation widths which are different for the two spin states of the compound nucleus. For these nuclides values are listed for both spin states.

8f-6. Infinite-dilution Resonance Integrals.¹ The neutron cross sections for most nuclides exhibit resonance structure. The incident neutron energy range in which

¹ We should like to express our appreciation to Dr. M. K. Drake, of the Gulf General Atomic Corporation (now at Brookhaven National Laboratory), for supplying the information contained in this section and in Table 8f-5.

the individual resonances can be observed varies from nuclide to nuclide; but for most of the heavier nuclides, this energy range begins at near-thermal neutron energies and extends to approximately 10 keV. The resonance integral is a quantity that is frequently used to characterize the magnitude of the neutron cross section for the resonance energy region. The resonance integral has been found to be particularly useful in characterizing the absorption cross section for materials used in reactor physics analysis.

When a resonance absorber is placed in a moderator at near-zero concentrations, the resonance absorption integral is not affected by energy self-shielding or by Doppler broadening. Under these conditions, the material absorbs neutrons in the slowing-down spectrum of the moderator. The resonance integral is expressed as

$$\text{R.I.} = \int_{E_c}^{E_{\max}} \sigma(E) \phi(E) dE$$

where $\sigma(E)$ is the neutron cross section as a function of energy E . In the case where the absorber is at near-zero concentrations in a moderator, the weighting function $\phi(E)$ (neutron flux distribution) is proportional to $1/E$ for neutron energies greater than a few tenths of an electron volt. The upper limit of the integral is generally taken as a few MeV. The lower-energy limit is generally taken as the cutoff, between where the neutron flux distribution can be treated as being $1/E$ and where a Maxwellian distribution can be used. In most experimental measurements of the resonance integral, E_c is determined by the type and thickness of the filter used to absorb the neutrons in the Maxwellian portion of the spectrum. Cadmium is the material generally used as the filter, and an appropriate thickness of the material results in a cutoff energy of 0.5 eV.

In Table 8f-5 are listed recommended infinite-dilution resonance integrals. The values given in this table have been taken from various sources. In most cases the recommended values have been taken from experimental integral measurements. In other cases the values have been obtained by integrating experimentally measured, differential cross-section data. Resonance integrals for several reaction mechanisms, i.e., (n,γ) , $(n, \text{fission})$, and $(n, \text{absorption})$, are included. The particular reaction mechanism is given in the Reaction column. In certain cases the (n,γ) reaction produces two or more different states of the residual nucleus, and this information is also given in the Reaction column. The recommended resonance integrals (R.I.) at infinite dilution are given in the final column. In all cases the cutoff energy E_c has been taken as 0.5 eV, and the upper energy limit E_{\max} has been taken to be 15 MeV. Also, the integrals given in Table 8f-5 contain the contribution from the $1/v$ part of the low-energy cross sections.

8f-7. Neutron Flux Standards. Because of the uncharged nature of the neutron, its direct detection is difficult. For many cross-section measurements a knowledge of the incident neutron flux, either absolute or relative, is required, and many techniques are employed to accomplish this end. For absolute flux measurements, techniques used include the production of known flux by means of source reactions (see Sec. 8f-9), the utilization of the reasonably well-known characteristics of the interactions of neutrons with protons (the $n-p$ interaction), and the invocation of certain well-determined cross sections as standards for measurement of other lesser-known cross sections. The $n-p$ interaction is, of course, only a special case of the last technique.

The total $n-p$ cross section has been measured to high precision at a number of neutron energies. These data have been fitted by an analytical form based on effective range theory. The resulting equation, which gives the total cross section σ_t in barns for an incident laboratory neutron energy E in MeV, seems to fit the high-

TABLE 8f-4. s -WAVE NEUTRON STRENGTH FUNCTIONS Γ_n^o/D , s -WAVE OBSERVED RESONANCE SPACINGS D_{obs} , AND s -WAVE AVERAGE RADIATION WIDTHS Γ_γ

Target nucleus A	$\Gamma_n^o/D \times 10^4$	$D_{obs} \text{ eV}$	$\Gamma_\gamma^o \text{ mV}$	Target nucleus A	$\Gamma_n^o/D \times 10^4$	$D_{obs} \text{ eV}$	$\Gamma_\gamma^o \text{ mV}$
					Z		
9 F	19	0.7	$(6 \pm 3) \times 10^4$	38 Sr	0.5	340	± 90
11 Na	23	0.8	$(2.7 \pm 1.4) \times 10^4$		0.65	± 0.3	$\pm 0.3) \times 10^3$
13 Al	27	0.9	$(4 \pm 2) \times 10^4$		0.5	± 0.1	200
16 S	32	1.2	$(2.9 \pm 0.9) \times 10^4$		0.30	± 0.08	± 60
17 Cl		0.65 ± 0.20			87	0.9	$(3.5 \pm 1.9) \times 10^4$
35	0.30 ± 0.15	$(1.3 \pm 0.4) \times 10^4$	500 $\pm 20^*$	39 Y	0.4	± 0.2	$(1.0 \pm 0.3) \times 10^3$
37	0.63 ± 0.20	$(1.3 \pm 0.4) \times 10^4$	1800 $\pm 200^*$	40 Zr	0.65	± 0.25	
18 Ar	36				90	1.4	$(4.5 \pm 1.6) \times 10^3$
19 K	39	1.3 ± 0.4	$(1.0 \pm 0.3) \times 10^4$		91	0.8	± 0.3
20 Ca	40	3.1	$(4.9 \pm 1.0) \times 10^4$		92	0.5	315 ± 85
42	2.2 ± 0.7	$(2.8 \pm 0.4) \times 10^4$			92	0.5	$(1.2 \pm 0.4) \times 10^3$
43	1.4 ± 0.6	$(3.3 \pm 0.6) \times 10^4$			94	1.5	$(2.4 \pm 0.9) \times 10^3$
44	2.7 ± 1.0	$(3.3 \pm 0.5) \times 10^4$			96	1.5	$(1.0 \pm 0.3) \times 10^3$
21 Sc	45	5.0 ± 0.9	$(1.3 \pm 0.4) \times 10^4$	41 Nb	0.4	± 0.1	220 $\pm 50^*$
22 Ti	46	3.5		42 Mo	0.6	± 0.15	170 ± 20
47	2.6 ± 1.1	$(3.0 \pm 0.6) \times 10^4$		92	1.0		
48	2.9 ± 0.8	$(2.6 \pm 0.4) \times 10^4$		94	0.5		
49	3.6 ± 1.4	$(2.2 \pm 0.4) \times 10^4$		95	0.55	± 0.22	
50	3.0 ± 0.8	$(4.0 \pm 1.0) \times 10^3$		96	0.8		
51	1.4	$(1.2 \pm 0.5) \times 10^4$		97	0.6	± 0.24	
52	4.5 ± 1.7	$(1.1 \pm 0.3) \times 10^4$		98	0.8	± 0.4	
53	4.2 ± 1.0	$(3.6 \pm 0.9) \times 10^3$	$\sim 1500^*$	100	0.9	430 ± 150	
54	4.0 ± 1.0	$(1.6 \pm 0.2) \times 10^4$	2900 $\pm 900^*$	43 Tc	0.45	± 0.18	
55	2.5 ± 1.0	$(4.4 \pm 0.8) \times 10^4$		99	0.3	± 0.15	
56	4.1 ± 1.0	$(3.0 \pm 0.7) \times 10^4$		101	0.4	± 0.2	
57	2.2 ± 0.9	$(2.3 \pm 0.4) \times 10^4$		102	0.4	± 0.2	
58	4.2 ± 1.0	$(2.1 \pm 0.8) \times 10^4$	450 $\pm 40^*$	45 Rh	0.43	± 0.15	
59	5.2 ± 1.7	$(2.5 \pm 0.4) \times 10^4$		103	26	± 8	
60	1.6 ± 0.5	$(2.9 \pm 0.4) \times 10^4$	1400 $\pm 200^*$	46 Pd	0.35	± 0.10	
61	3.0 ± 1.0	$(8 \pm 3) \times 10^3$	2000 $\pm 1000^*$	105	0.35	± 0.15	
62	3.5 ± 1.0	960 ± 210	450 ± 50	108	30	± 3	
63				47 Ag	0.45	± 0.1	

28 Ni	2.4	± 0.9	$(2.7 \pm 0.5) \times 10^4$	48 Cd	107	0.4 ± 0.1	30 ± 10	141	± 4
	58	± 0.7	$(2.3 \pm 0.4) \times 10^4$		109	0.8 ± 0.3	13 ± 3	133	± 3
	60	± 0.6	$(2.4 \pm 0.6) \times 10^4$		110	0.4 ± 0.15	>45	130	$\pm 40^*$
	61	± 0.6	$(1.9 \pm 0.3) \times 10^4$		111	0.35	25 ± 5	95	$\pm 20^*$
	62	± 0.8	$(2.8 \pm 0.4) \times 10^4$		112	0.45	200 ± 50	90	$\pm 30^*$
	64	± 0.7	$(1.2 \pm 0.3) \times 10^4$	49 In	113	0.4	25 ± 5	110	$\pm 5^*$
29 Cu	1.9	± 0.8	$(1.7 \pm 0.3) \times 10^4$		114	0.6	160 ± 50	150	$\pm 50^*$
	63	± 0.7	$(1.7 \pm 0.3) \times 10^4$	49 In	113	0.4	5.5 ± 2.0	70	$\pm 20^*$
	65	± 0.6	$(2.6 \pm 0.9) \times 10^4$		115	0.3	0.7 ± 2.0	76	$\pm 5^*$
30 Zn	64	± 0.6	$(5.0 \pm 1.3) \times 10^4$	50 Sn	112	0.2	0.1		
	66	± 1.5	600 ± 300		114	0.5	0.2	25	± 7
	67	± 1.1	$400 \pm 70^*$		114	0.7	150 ± 60	110	$\pm 30^*$
	68	± 0.8	$180 \pm 30^*$		115	0.3	50 ± 30	70	$\pm 30^*$
31 Ga	69	± 0.5	$210 \pm 50^*$		116	0.26 ± 0.05	150 ± 20	70	± 15
	71	± 1.5	$350 \pm 110^*$		117	0.16 ± 0.03	25 ± 5	70	± 15
32 Ge	70	± 0.7	$(1.7 \pm 0.3) \times 10^4$		118	0.4 ± 0.2	180 ± 50	79	$\pm 14^*$
	72	± 0.5	$(2.1 \pm 0.4) \times 10^4$		119	0.08 ± 0.03	30 ± 8	70	$\pm 30^*$
	73	± 0.7	$(8.5 \pm 1.0) \times 10^4$		120	0.12 ± 0.06	200 ± 70	100	$\pm 50^*$
	74	± 0.8	$(8 \pm 1) \times 10^4$		122	0.4	400 ± 200	130	$\pm 60^*$
	76	± 1.8	290 ± 20	51 Sb	124	0.10	400 ± 200		
33 As	75	$\{ 1.0 \pm 0.3$	$260 \pm 50^*$		121	0.4 ± 0.1	14 ± 4	92	± 4
		$\{ 2.5 \pm 0.6 \dagger$	$230 \pm 40^*$		123	0.5	28 ± 12	90	± 20
34 Se	74	± 0.6	370 ± 70	52 Te	122	0.5	0.2	130	± 15
	76	± 0.8	700 ± 150		123	0.8	0.2	130	± 5
	77	± 0.5	100 ± 25		124	1.0	0.2	26	± 5
	78	± 0.4	1000 ± 200		125	0.7	0.2	147	± 11
	80	± 0.8	1200 ± 400		126	0.49 ± 0.10	38 ± 4	150	$\pm 80^*$
	82	± 1.0	$(7 \pm 1) \times 10^3$		128	0.30 ± 0.10	210 ± 20		
35 Br	79	$\{ 0.9 \pm 0.3$	290 ± 20	53 I	127	0.6 ± 0.1	13.0 ± 0.5		
		$\{ 1.9 \pm 0.4 \dagger$	340 ± 30		129	0.3	31 ± 10		
	81	± 0.6	300 ± 30	54 Xe	129	1.0	40 ± 15	120	$\pm 7^*$
36 Kr	80	\dots	$400 \pm 90^*$		130	2.0 ± 0.7	31 ± 16	113	$\pm 8^*$
	83	\dots	$220 \pm 60^*$		131	$1.5 \pm 20^*$	145 ± 400	91	$\pm 1^*$
37 Rb	85	± 0.4	180 ± 30		135	$1.1 \pm 30^*$	1600 ± 400		
	87	± 0.4	215 ± 20						

* Based on data for only one or two resonances (sometimes computed from thermal-capture cross sections or resonance-capture integrals).

TABLE 8f-4. *s*-WAVE NEUTRON STRENGTH FUNCTIONS Γ_n^o/D , *s*-WAVE OBSERVED RESONANCE SPACINGS D_{obs} , AND *s*-WAVE AVERAGE RADIATION WIDTHS Γ_r (*Continued*)

Target nucleus Z	$\Gamma_n^o/D \times 10^4$	D_{obs} eV	Γ_r mV	Target nucleus Z	$\Gamma_n^o/D \times 10^4$	D_{obs} eV	Γ_r mV
65 Cu	133	0.7 ± 0.1	20	120	1.6 ± 20*	179	4.5 ± 0.7
66 Ba	130	3.2	150	107	0.3 ± 5	180	100 ± 40
135	0.8 ± 0.3	35	180	181	2.0 ± 1.0	180	30 ± 5*
136	(4 ± 2) × 10 ³	180	182	2.4 ± 0.4	182	56 ± 2
137	0.34	400	100	1.7	4.4 ± 0.4	182
138	1.8 ± 0.6	(10 ± 4) × 10 ³	99	74 W	2.7 ± 0.5	180	30 ± 7
57 La	138	1.0 ± 0.5	23	80	1.0 ± 0.5	182	56 ± 2
139	0.7 ± 0.2	90	20	80	2.6 ± 0.5	183	74 ± 3
58 Ce	0.8	80	2.4 ± 0.5	183	68 ± 3
140	1.0	(3 ± 1) × 10 ³	80	2.6 ± 0.8	184	62 ± 3
142	1.2 ± 0.4	(1.0 ± 0.2) × 10 ³	82	75 Re	2.2 ± 0.5	186	15 ± 4
59 Pr	141	2.1 ± 0.4	51	82	2.4 ± 0.5	186	14 ± 3
60 Nd	2.5 ± 0.5	82	2.0 ± 0.5	185	13 ± 3
142	0.6 ± 0.3	1000	± 250	82	2.8 ± 0.6	185	53 ± 2
143	4.3 ± 1.4	38	± 6	82	2.1 ± 0.7	187	54 ± 2
144	4.8 ± 2.0	520	± 70	76	2.4 ± 0.5	187
145	3.0 ± 0.7	19	± 3	78	2.0 ± 0.5	189	90 ± 7
146	4.5 ± 1.9	310	± 40	58	2.2 ± 0.5	189
148	3.6 ± 1.1	220	± 20	55	2.1 ± 0.8	191	71 ± 2*
150	2.0 ± 0.8	230	± 30	96	2.0 ± 0.5	193	87 ± 1*
61 Pm	147	4.2 ± 1.8	4.0 ± 1.0	84	2.0 ± 0.5	192	52 ± 8*
62 Sm	2.3	65	1.7 ± 0.3	194	70 ± 15*
147	4.5	8.0	± 1.7	61	2.0 ± 0.7	195	93 ± 10
149	3.0 ± 1.0	2.4	± 0.6	62	1.9 ± 0.4†	196	118 ± 6†
151	3.5 ± 1.9	2.3	± 0.4	62	2.0 ± 0.5	196	120 ± 20*
152	2.7 ± 0.8	53	± 8	65	2.1 ± 0.6	198	150 ± 30*
154	1.9 ± 0.7	125	± 20	75	2.0 ± 0.5	198	125 ± 4
63 Eu	151	2.9 ± 0.5	1.04 ± 0.07	95	0.9 ± 0.4	197	220 ± 100*
153	2.2 ± 0.7	1.45 ± 0.12	94	94	1.4 ± 0.5	196	135 ± 15
64 Gd	1.5 ± 0.3	90	>50	1.0

... for only one or two resonances (sometimes computed from thermal-capture cross sections or resonance-capture integrals).

TABLE 8f-5. TABLE OF INFINITE-DILUTION RESONANCE INTEGRALS

Target nucleus Z A	Reaction	Resonance integral, barns	Target nucleus Z A	Reaction	Resonance integral, barns
1 H 1	n, γ	0.149 ± 0.001	81	$(n, \gamma)^{stat} Br(6.2 \text{ min})$ $(n, \gamma)^{sys} Br(36 \text{ hr})$	34 ± 2
2 He 2	n, γ Abs.	$(0.26 \pm 0.02) \times 10^{-3}$ $(3.1 \pm 1.0) \times 10^{-3}$	81	n, γ	7 ± 1
3 Li 3	n, p Abs.	2.397 ± 10	36 Kr	n, γ	150 ± 50
6	n, α	32 ± 1	84	n, γ	5 ± 2
6	n, γ	430 ± 10	85	n, γ	14 ± 7
7	n, γ	$(20 \pm 6) \times 10^{-4}$	86	n, γ	0.05 ± 0.02
7	n, γ	$(17 \pm 3) \times 10^{-3}$	37 Rb	n, γ	5 ± 2
10 Be 5	n, γ Abs.	$(4.5 \pm 0.6) \times 10^{-3}$	85	n, γ	6 ± 2
10 B 10	n, α	341 ± 1	87	n, γ	3 ± 1
10	n, γ	1.725 ± 6	88	n, γ	14 ± 4
11	n, γ	0.23 ± 0.1	89	n, γ	0.06 ± 0.03
6 C 7	n, γ	$(25 \pm 10) \times 10^{-3}$	39 Y	n, γ	2 ± 1
N 14	n, γ	$(1.3 \pm 0.2) \times 10^{-3}$	40 Zr	n, γ	0.9 ± 0.2
14	n, p	1.03 ± 0.03	90	n, γ	1.20 ± 0.1
14	n, γ	1.00 ± 0.03	91	n, γ	0.25 ± 0.05
8 O 9	n, γ Abs.	$(34 \pm 4) \times 10^{-3}$ $(0.08 \pm 0.02) \times 10^{-3}$	92	n, γ	7.3 ± 1.0
F 19	n, γ	0.25 ± 0.1	94	n, γ	0.6 ± 0.2
19	n, γ	$(25 \pm 5) \times 10^{-3}$	96	n, γ	0.3 ± 0.1
10 Ne	n, γ	$(17 \pm 5) \times 10^{-3}$	41 Nb	n, γ	3.5 ± 1.5
11 Na 22	n, γ	$(2.0 \pm 0.3) \times 10^{-3}$	94	n, γ	9.0 ± 0.5
23	n, γ	0.314 ± 0.01	42 Mo	n, γ	160 ± 30
12 Mg	n, γ	0.35 ± 0.1	92	n, γ	25 ± 2
13 Al 27	n, γ Abs.	0.07 ± 0.02	94	n, γ	0.53 ± 0.04
27	n, γ	0.28 ± 0.01	95	n, γ	0.95 ± 0.05
14 Si	n, γ Abs.	0.13 ± 0.01	96	n, γ	110 ± 5
14	n, γ	0.54 ± 0.06	97	n, γ	25 ± 2
15 P 31	n, γ Abs.	0.09 ± 0.02	98	n, γ	16 ± 1
31	n, γ	0.30 ± 0.05	100	n, γ	7.3 ± 0.5
16 S	n, γ Abs.	0.09 ± 0.01	43 Tc	n, γ	4.8 ± 0.5
17 Cl	n, γ Abs.	1.3 ± 0.2	44 Ru	n, γ	190 ± 20
	n, γ	0.4 ± 0.1	96	n, γ	60 ± 25
	n, γ	13.5 ± 1.0	98	n, γ	6 ± 1
	n, γ	13.0 ± 1.0	99	n, γ	10 ± 5
	n, γ	12 ± 2	100	n, γ	210 ± 20

TABLE 8f-5. TABLE OF INFINITE-DILUTION RESONANCE INTEGRALS (*Continued*)

Target nucleus <i>Z</i> <i>A</i>	Reaction	Resonance integral, burns	Target nucleus <i>Z</i> <i>A</i>	Reaction	Resonance integral, burns
51 Sb	119 <i>n, γ</i>	5 ± 1	63 Eu	151	2,300 ± 300
	120 <i>n, γ</i>	2.0 ± 0.5		153	3,300 ± 300
	122 <i>n, γ</i>	1.5 ± 0.5		154	1,450 ± 200
	124 <i>n, γ</i>	1.3 ± 2		155	950 ± 300
52 Te	121 <i>n, γ</i>	170 ± 15	64 Gd	154	0,000 ± 1,000
	123 <i>n, γ</i>	200 ± 10		155	430 ± 40
	124 <i>n, γ</i>	125 ± 10		155	500 ± 200
	125 <i>n, γ</i>	54 ± 5		155	1,730 ± 200
53 I	120 <i>n, γ</i>	2.0 ± 0.5	65 Tb	156	110 ± 10
	122 <i>n, γ</i>	65 ± 5		157	790 ± 50
	123 <i>n, γ</i>	5,600 ± 500		158	70 ± 7
	124 <i>n, γ</i>	4 ± 1		160	1.3 ± 2
54 Xe	125 <i>n, γ</i>	19 ± 2	66 Dy	159	400 ± 20
	126 <i>n, γ</i>	10 ± 1		158	1,425 ± 200
	128 <i>n, γ</i>	1.5 ± 0.2		160	100 ± 50
	130 <i>n, γ</i>	0.35 ± 0.05		161	1,100 ± 200
55 Cs	127 <i>n, γ</i>	1.54 ± 5	67 Ho	162	1,190 ± 150
	129 <i>n, γ</i>	35 ± 5		163	2,575 ± 300
	131 <i>n, γ</i>	8 ± 4		164	1,650 ± 200
	124 <i>n, γ</i>	265 ± 50		165	380 ± 30
56 Sr	128 <i>n, γ</i>	3,600 ± 500	68 Er	162	700 ± 30
	129 <i>n, γ</i>	300 ± 100		164	780 ± 60
	130 <i>n, γ</i>	12 ± 3		166	440 ± 40
	131 <i>n, γ</i>	840 ± 50		167	90 ± 10
57 Y	132 <i>n, γ</i>	2.5 ± 0.5	69 Tm	168	115 ± 10
	133 <i>n, γ</i>	160 ± 20		170	3,150 ± 200
	134 <i>n, γ</i>	2 ± 1		169	38 ± 4
	135 <i>n, γ</i>	7600 ± 500		70 Yb	45 ± 4
58 Ba	136 <i>n, γ</i>	1.2 ± 2	(n,γ) ^{138m} Cs	168	1,550 ± 100
	137 <i>n, γ</i>	35 ± 3		170	185 ± 15
	133 <i>n, γ</i>	385 ± 40		171	31,000 ± 3,000
	133 <i>n, γ</i>	420 ± 40		172	350 ± 40
59 La	135 <i>n, γ</i>	60 ± 5	(n,γ) ¹³⁴ Cs	173	340 ± 30
	137 <i>n, γ</i>	1.0 ± 0.5		173	28 ± 3
					400 ± 40

56 Ba	130	<i>n, γ</i>	9 ± 2	36 ± 4
	132	<i>n, γ</i>	15 ± 3	14 ± 2
	134	<i>n, γ</i>	6 ± 3	670 ± 70
	135	<i>n, γ</i>	15 ± 5	660 ± 70
	136	<i>n, γ</i>	100 ± 20	950 ± 100
	137	<i>n, γ</i>	18 ± 2	2,000 ± 200
	138	<i>n, γ</i>	5 ± 1	450 ± 50
	140	<i>n, γ</i>	0.25 ± 0.05	800 ± 80
	57 La	<i>n, γ</i>	14 ± 2	7,300 ± 200
	138	<i>n, γ</i>	12.3 ± 1.0	1,900 ± 200
	139	<i>n, γ</i>	330 ± 30	625 ± 50
	140	<i>n, γ</i>	12 ± 1	45 ± 5
	58 Ce	<i>n, γ</i>	70 ± 5	740 ± 40
	140	<i>n, γ</i>	0.45 ± 0.05	100 ± 30
	142	<i>n, γ</i>	2.5 ± 0.5	740 ± 40
	144	<i>n, γ</i>	2.6 ± 0.3	350 ± 30
	141	<i>n, γ</i>	18.3 ± 1.0	10 ± 10
	143	<i>n, γ</i>	190 ± 40	590 ± 10
	144	<i>n, γ</i>	60,000 ± 30,000	380 ± 15
	60 Nd	<i>n, γ</i>	45 ± 5	13 ± 2
	142	<i>n, γ</i>	12 ± 2	490 ± 50
	143	<i>n, γ</i>	115 ± 10	850 ± 50
	144	<i>n, γ</i>	10 ± 2	1,770 ± 100
	145	<i>n, γ</i>	260 ± 15	310 ± 20
	146	<i>n, γ</i>	12 ± 2	210 ± 20
	148	<i>n, γ</i>	18 ± 1	250 ± 30
	150	<i>n, γ</i>	16 ± 2	760 ± 100
	147	<i>n, γ</i>	2,300 ± 400	2,050 ± 150
	147	<i>(n, γ)^{148m}</i> Pm	1,200 ± 300	3,100 ± 200
	147	<i>(n, γ)¹⁴⁸</i> Pm	1,100 ± 300	1,400 ± 100
	148m	<i>n, γ</i>	30,000 ± 10,000	140 ± 10
	148g	<i>n, γ</i>	40,000 ± 10,000	80 ± 30
	62 Sm	<i>n, γ</i>	1,400 ± 150	90 ± 10
	144	<i>n, γ</i>	10 ± 5	14 ± 2
	147	<i>n, γ</i>	590 ± 20	380 ± 20
	148	<i>n, γ</i>	20 ± 10	5 ± 2
	149	<i>n, γ</i>	3,200 ± 100	50 ± 5
	160	<i>n, γ</i>	350 ± 50	1,565 ± 40
	151	<i>n, γ</i>	2,450 ± 300	90 ± 10
	162	<i>n, γ</i>	3,100 ± 100	1,350 ± 200
	154	<i>n, γ</i>	40 ± 20	70 ± 10
			198	
			79 Au	197
			80 Hg	196
			198	

TABLE 8f-5. TABLE OF INFINITE-DILUTION RESONANCE INTEGRALS (Continued)

Target nucleus Z A	Reaction	Resonance integral, barns	Target nucleus Z A	Reaction	Resonance integral, burns
199	n, γ	410 ± 50	238	Fiss.	750 ± 250
200	n, γ	20 ± 5	238	Abs.	$1,500 \pm 500$
201	n, γ	40 ± 10	239	n, γ	450 ± 300
202	n, γ	6 ± 2	94 Pu	n, γ	145 ± 8
81 Tl	203	12 ± 2	238	Fiss.	24 ± 4
205	n, γ	40 ± 5	238	Abs.	169 ± 10
82 Pb	204	0.7 ± 0.1	239	n, γ	190 ± 10
	206	0.18 ± 0.02	239	Fiss.	310 ± 15
	207	2.7 ± 0.3	239	Abs.	500 ± 20
	208	0.12 ± 0.02	240	n, γ	$8,200 \pm 600$
	209	0.45 ± 0.05	241	n, γ	160 ± 20
	83 Bi	0.015 ± 0.005	241	Fiss.	590 ± 30
89 Ac	227	n, γ	241	Abs.	750 ± 40
90 Th	230	n, γ	242	n, γ	$1,200 \pm 100$
	232	n, γ	241	n, γ	$2,400 \pm 800$
	233	n, γ	241	$(n, \gamma)^{232m} Am$	300 ± 100
	91 Pa	231	n, γ	$(n, \gamma)^{231} Am$	$2,100 \pm 700$
	233	n, γ	241	Fiss.	20 ± 5
92 U	232	n, γ	242m	Fiss.	$1,600 \pm 200$
234	Fiss.	84 ± 2	243	n, γ	$2,300 \pm 400$
	232	500 ± 200	243	$(n, \gamma)^{244m} Am$	$2,200 \pm 400$
	233	510 ± 50	243	$(n, \gamma)^{244} Am$	110 ± 20
	233	890 ± 50	244	n, γ	650 ± 60
	233	240 ± 40	244	Fiss.	20 ± 4
	234	320 ± 40	244	Abs.	670 ± 60
	232	Abs.	245	n, γ	250 ± 50
	233	n, γ	245	Fiss.	500 ± 100
	233	Fiss.	245	Abs.	750 ± 100
	233	Abs.	246	n, γ	250 ± 50
	234	n, γ	248	n, γ	350 ± 50
	235	n, γ	245	Fiss.	$1,200 \pm 200$
	235	Fiss.	245	Abs.	$5,300 \pm 500$
	235	Abs.	246	n, γ	$1,000 \pm 100$
	236	n, γ	248	n, γ	$3,500 \pm 600$
	238	n, γ	249	n, γ	
	237	n, γ	250	n, γ	
	237	Fiss.	251	n, γ	
	237	Abs.	99 Es	n, γ	
	238	n, γ	253	n, γ	

precision cross-section measurements to much better than 1 percent. It can be expressed as follows:

$$\sigma_r = 3\pi[1.206E + (-1.860 + 0.0941491E + 0.000130658E^2)^{-1}]^{-1} + \pi[1.206E + (0.4223 + 0.1300E)^{-1}]^{-1} \quad 0 \leq E \leq 40 \text{ MeV}$$

For the angular distribution in n - p scattering, the apparent isotropy of the scattering in the center-of-mass system up to approximately 10 MeV leads to the equation for the laboratory differential cross section at a laboratory scattering angle θ :

$$\sigma(\theta) = \frac{\sigma_r}{\pi} \cos \theta \quad 0 \leq E \lesssim 10 \text{ MeV}$$

For further discussion of these n - p relations, see the chapters by J. L. Gammel and by J. E. Perry, Jr., in "Fast Neutron Physics." The constants in the σ_r equation are those of Marion and Young in "Nuclear Reaction Analysis," published by North-Holland Publishing Company, Amsterdam, 1968.

The use of well-measured cross sections as standards against which newer measurements are made occurs for all energy neutrons from thermal to very high energies. For cross sections using a thermal spectrum, some much-used 2,200 m/sec standard cross section values are shown in Table 8f-6.

TABLE 8f-6. 2,200-M/SEC STANDARD VALUES FOR CROSS SECTIONS
USING A THERMAL SPECTRUM

Target	Reaction	Cross section, barns
He ³	(n,p)	5.327 ± 10
Li ⁶	(n,t)	950 ± 15
B ¹⁰	(n,α)	3,836 ± 9
Co ⁵⁹	(n,γ)	37.2 ± 0.3
Au ¹⁹⁷	(n,γ)	98.8 ± 0.3
U ²³⁵	(n,f)	580.2 ± 1.8
Pu ²³⁹	(n,f)	741.6 ± 3.1

For neutron energies in the resonance region ($1 \text{ eV} \lesssim E \lesssim 10 \text{ keV}$), capture or fission data are usually made absolute either by measurements of the integrated flux over a particular well-determined resonance (or group of resonances) in a standard material or by normalization to other measurements on resonances in the nucleus under study. In addition, some reaction cross sections whose variations are monotonic and well-defined are used as detectors and provide excellent relative standards and occasionally adequate absolute standards. Examples are the He³(n,p)T, the Li⁶(n,t)He⁴, and the B¹⁰(n,α)Li⁷ reactions, all of which vary as $1/\sqrt{E}$ below 10 keV.

For fast neutrons, flux measurements are made using a variety of total cross sections which are either constant or monotonically varying in the region of interest. (One, of course, is the n - p cross section, mentioned above.) Also various reaction cross sections can be used under the same conditions. The three reactions mentioned above for He³, Li⁶, and B¹⁰ continue their $1/\sqrt{E}$ behavior above 10 keV and are used up to energies where their energy variation is known to sufficient accuracy for the problem at hand. Some (n,γ) and (n,f) cross sections can be used to higher energies, though they are not usually known to the accuracies of the light-target reactions. Threshold reactions (see Sec. 8f-8) are useful for flux measurements on broad-energy-spectrum sources; and many (n,p), (n,α), and (n,2n) cross sections, measured near 14 MeV, have served as standards for subsequent 14-MeV measurements.

Curves showing the variation of $H^1(n,n)H^1$ (the $n-p$ total cross section), $He^3(n,p)T$, $Li^6(n,t)He^4$, and $B^{10}(n,\alpha)Li^7$ above 100 eV are shown in Fig. 8f-4, reproduced from "Nuclear Reaction Analysis" by J. B. Marion and F. C. Young. (We appreciate the permission granted by the authors and publisher to use this figure.)

8f-1. Threshold Reactions. Many nuclear reactions resulting from the bombardment of nuclei with neutrons have negative Q values and thus have an energetic threshold below which the reaction cannot occur. When this threshold energy is exceeded, it is found that the cross section rises rapidly, sometimes showing considerable structure superposed on this underlying increase. Beyond a certain energy, competition with other energetically possible reactions leads to a decreasing rise and an eventual fall in the cross section. When the resulting residual nuclei are radioactive and have convenient lifetimes and decay characteristics, the presence of the threshold offers a means of using the reaction as a rough spectrometer in a broad neutron spectrum.

Many reactions have been used as threshold detectors in experimental measurements. Some of the more common (n,p) , (n,α) , and $(n,2n)$ excitation functions used for this purpose are shown in Figs. 8f-5 to 8f-9. Most of the measurements were made with insufficient energy resolution to detect whatever fine structure might exist, but their use as detectors for broad-spectrum sources achieves the same integration effect.

For a detailed description of the characteristics and use of many threshold detectors, see chap. IV, C, by P. R. Byerly, Jr., in "Fast Neutron Physics," part I.

8f-9. Fast-neutron Source Reactions. The production of monoenergetic beams of fast neutrons ($E \gtrsim 1$ keV) is usually achieved by the interactions of light charged particles, using cyclotrons, cascade generators, or electrostatic accelerators to provide high-quality energy precision and variability. The energy of a neutron beam will depend upon the energy of the incident charged particles, the Q of the reaction, the masses of the incident and target nuclei, and the neutron emission angle. An energy "spread" of the neutron beam results from such considerations as the energy spread of the incident particles, the thickness of the target materials, and the angular spread caused by the geometric size of the observation apparatus. The kinematics of these reactions are well defined and are best described in chap. I, B, by J. Monahan, in "Fast Neutron Physics" part I.

The monoenergetic character of source reactions is only approximate, since complex-particle breakup or excitation of higher states in the product nucleus can contribute groups of neutrons with lower energies than those of the primary group. For the common source reactions the characteristics of the lower-energy neutrons are known well enough for appropriate corrections to be made, or else the energy separation from the primary group is sufficiently great for straightforward energy discrimination.

The four most used fast-neutron source reactions are the $Li^7(p,n)Be^7$, $T(p,n)He^3$, $D(d,n)He^3$, and $T(d,n)He^4$ reactions. With the high precision available on proton and deuteron energies with electrostatic generators, good-quality neutron beams can be produced with energies from a few keV up to approximately 30 MeV. Most measurements with these reactions are performed with neutrons emitted at 0 deg with respect to the incident-beam direction, since yields are higher and polarization effects are avoided. Exceptions to this rule include the use of back-angle beams near the threshold of the $Li^7(p,n)$ reaction in order to obtain the lowest possible energies, the use of beams at 90 deg from the $T(d,n)$ reaction with low-energy cascade generators in order to enhance the detection of the associated He^4 particle, and for polarization measurements when advantage is taken of the source-reaction polarization.

Figure 8f-10 shows the variation of the neutron energy with incident charged-particle energy at 0 deg for the four reactions. In addition, the energy of neutrons resulting from leaving Be^7 in its first excited state of 431 keV energy in the $Li^7(p,n)$ reaction is shown, as well as the 90 deg energy variation of the $T(d,n)$ reaction for low-

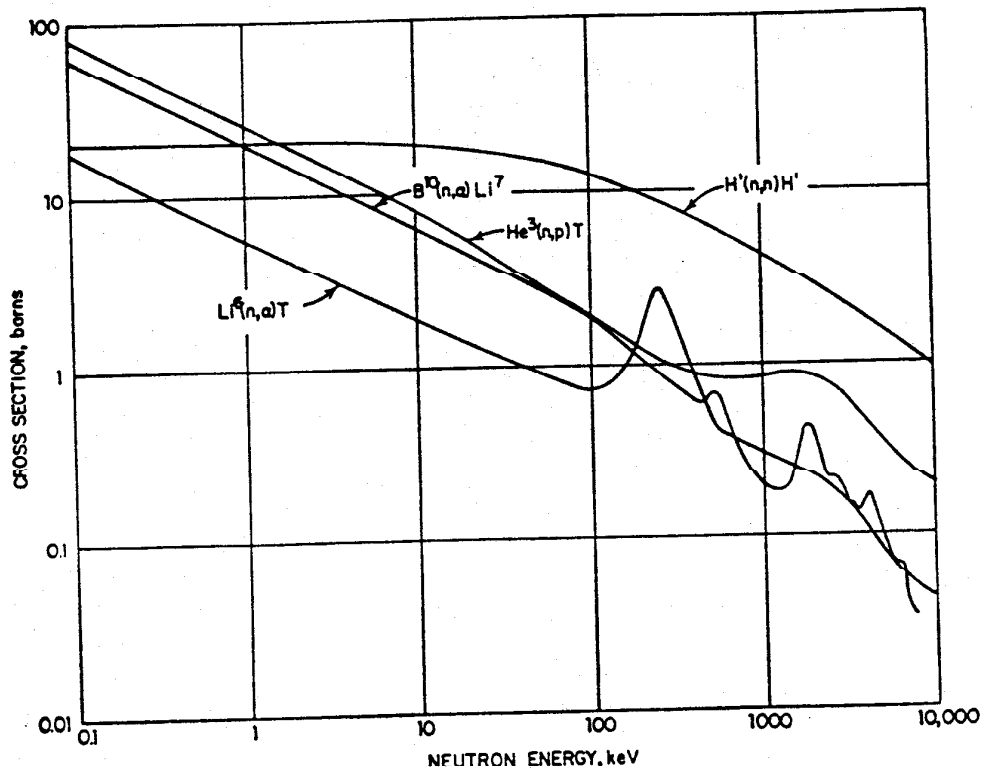


FIG. 8f-4. Variation of the cross section for $H^1(n,n)$, $He^3(n,p)$, $Li^6(n,t)$, and $B^{10}(n,\alpha)$ reactions for the neutron energy range 100 eV to 10 MeV.

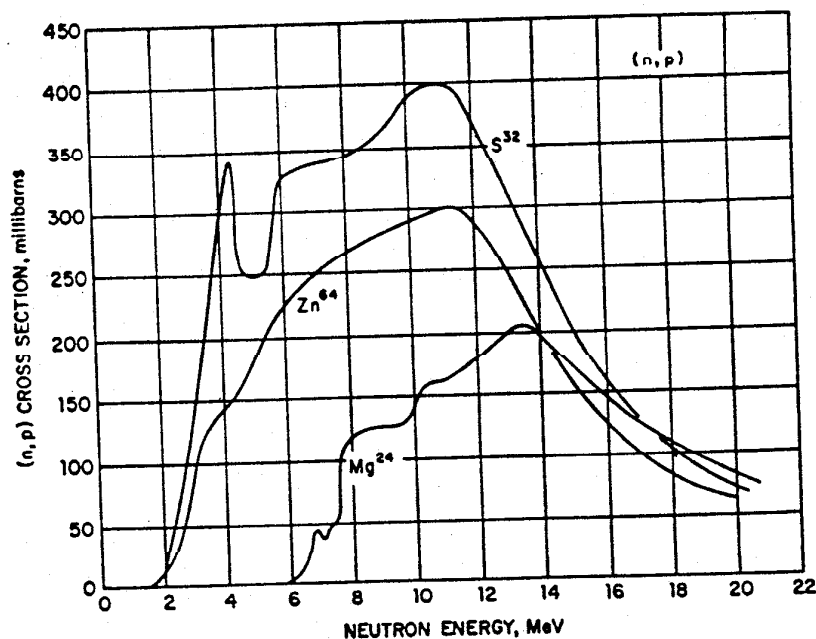


Fig. 8f-5. Variation of Mg^{24} , S^{32} , and $Zn^{64}(n,p)$ reaction cross sections from threshold to 20 MeV.

NUCLEAR PHYSICS

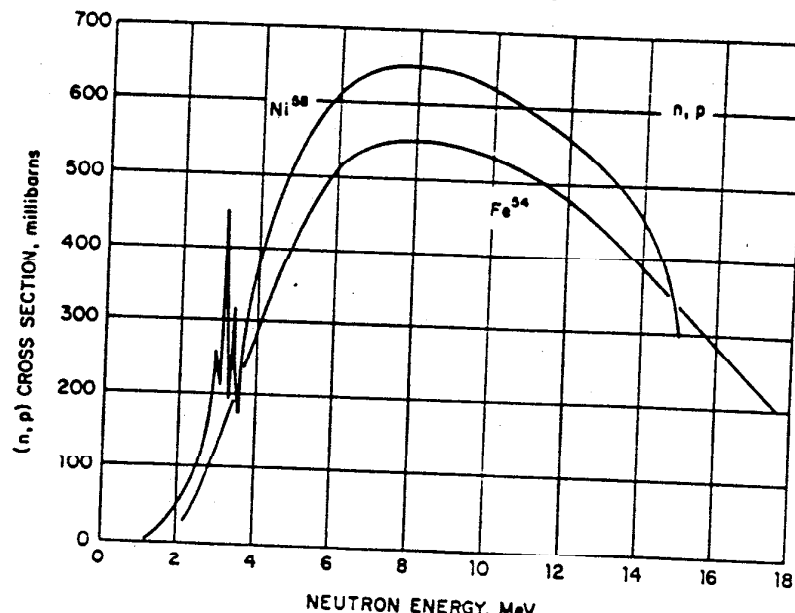


FIG. 8f-6. Variation of Fe^{54} and $\text{Ni}^{58}(n,p)$ reaction cross sections from threshold to 15 MeV.

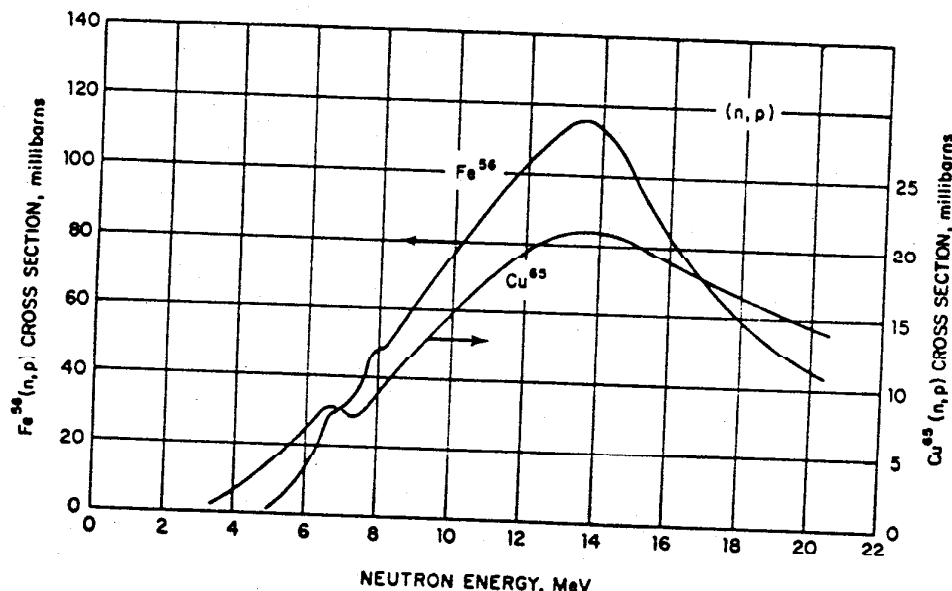


FIG. 8f-7. Variation of Fe^{56} and $\text{Cu}^{65}(n,p)$ reaction cross sections from threshold to 20 MeV.

energy deuterons. The energies have been calculated in a proper relativistic computation, but values cannot be obtained with high precision from this figure. Tables of values can be found in the appropriate chapters of "Fast Neutron Physics" part I. More extensive tables of energies can be found for the $\text{Li}^7(p,n)$ reaction in ANL-5219 (1954) by A. S. Langsdorf, Jr., J. E. Monahan, and W. A. Reardon; and for the three hydrogen-source reactions in AECU-3118 (1956) by L. Blumberg and S. I. Schlesinger.

The $\text{Li}^7(p,n)$ reaction has a Q value of -1.644 MeV with a corresponding threshold energy of 1.881 MeV. At a threshold energy of 2.378 MeV a second group of neutrons becomes energetically possible, owing to reactions in which the product Be^7 nucleus is

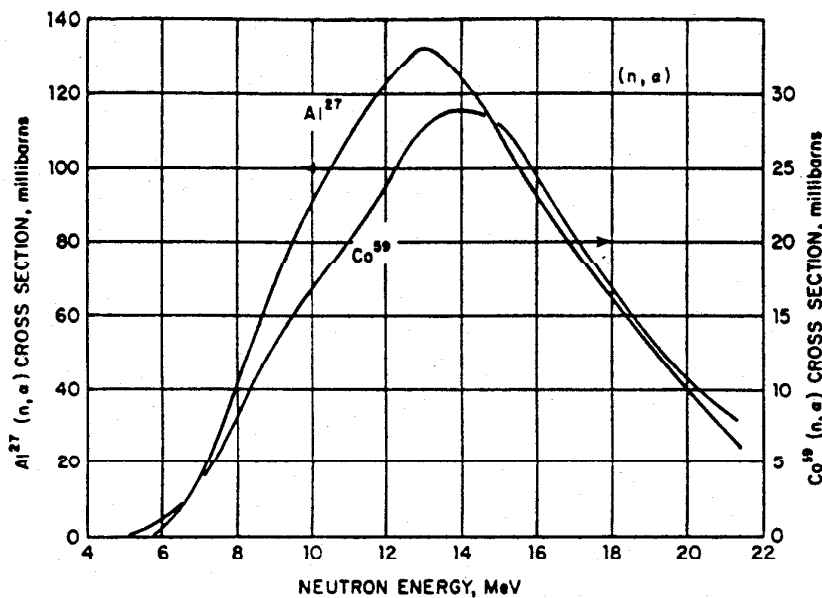


FIG. 8f-8. Variation of Al^{27} and $\text{Co}^{59}(n,\alpha)$ reaction cross sections from threshold to 21 MeV.

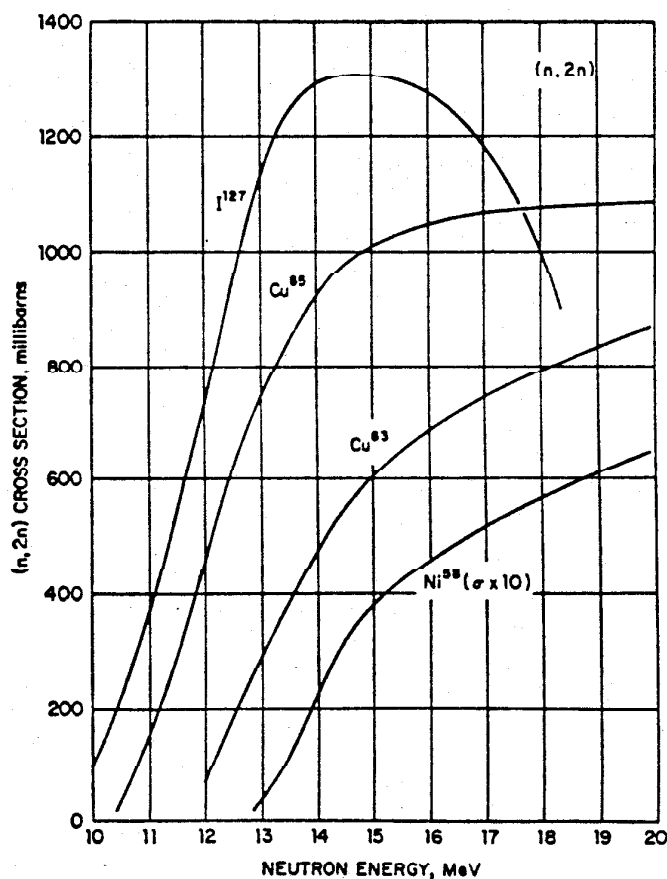


FIG. 8f-9. Variation of Ni^{58} , Cu^{63} , Cu^{65} , and $\text{I}^{127}(n,2n)$ reaction cross sections from threshold to 20 MeV. Note the multiplication of the true Ni^{58} cross section by 10 for plotting purposes.

left in its 431-keV first excited state. Because of the center-of-mass motion of the system, the laboratory neutron energy is a double-valued function of the proton energy near threshold. At threshold, all neutrons are emitted at 0 deg with an energy of 30 keV. When the 0 deg neutron energy reaches ≈ 120 keV, the double-valued character disappears. The laboratory 0 deg production cross section for this reaction as well as for the (p,n') reaction to the Be^7 431-keV state is shown in Fig. 8f-11. The

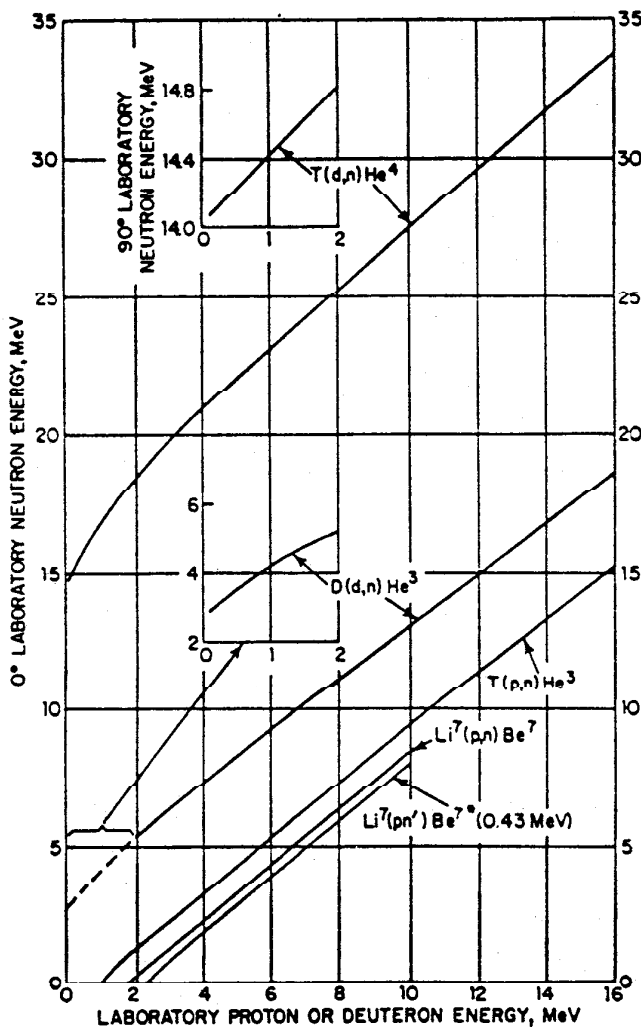


FIG. 8f-10. Variation of the laboratory neutron energy at 0 deg with incident charged-particle energy for the neutron source reactions $\text{Li}^7(p,n)$, $\text{T}(p,n)$, $\text{D}(d,n)$, and $\text{T}(d,n)$. Also shown is the same variation for the contaminant $\text{Li}^7(p,n')$ reaction and the neutron energy at 90 deg for the low-energy end of the $\text{T}(d,n)$ reaction.

latter curve, along with the neutron energies for this reaction (Fig. 8f-10), can be used to make corrections to experimental data taken with the primary neutron group.

The $\text{T}(p,n)\text{He}^3$ reaction is generally used to produce neutrons of energy greater than ≈ 700 keV, since the appearance of the second group in $\text{Li}^7(p,n)$ complicates use of that reaction to produce higher-energy neutrons. The Q value is -0.764 MeV, with a corresponding threshold energy of 64 keV. The laboratory 0 deg production cross section is shown in Fig. 8f-12. A possible contamination of the monoenergetic char-

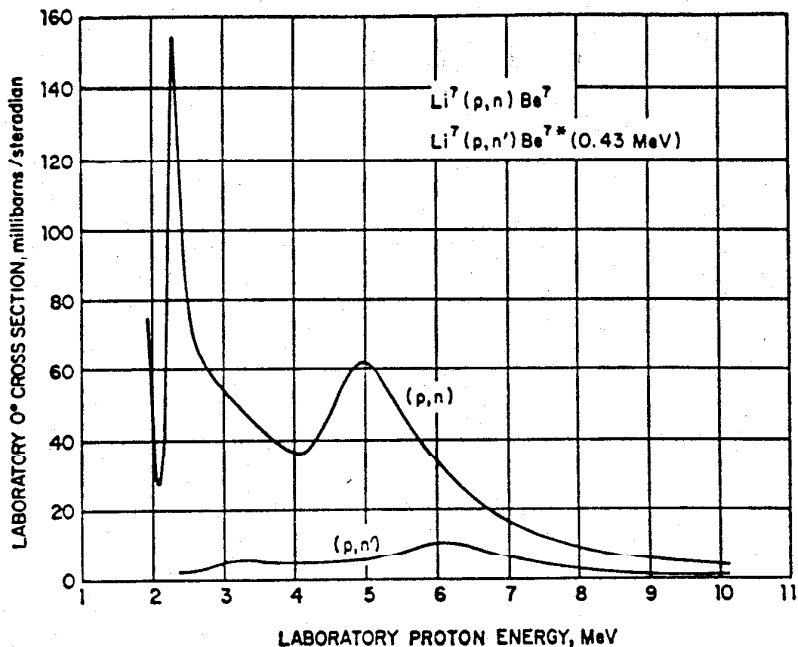


FIG. 8f-11. The laboratory 0-deg production cross section for the $\text{Li}^7(\text{p},\text{n})$ neutron source reaction and for the $\text{Li}^7(\text{p},\text{n}')$ contaminant reaction.

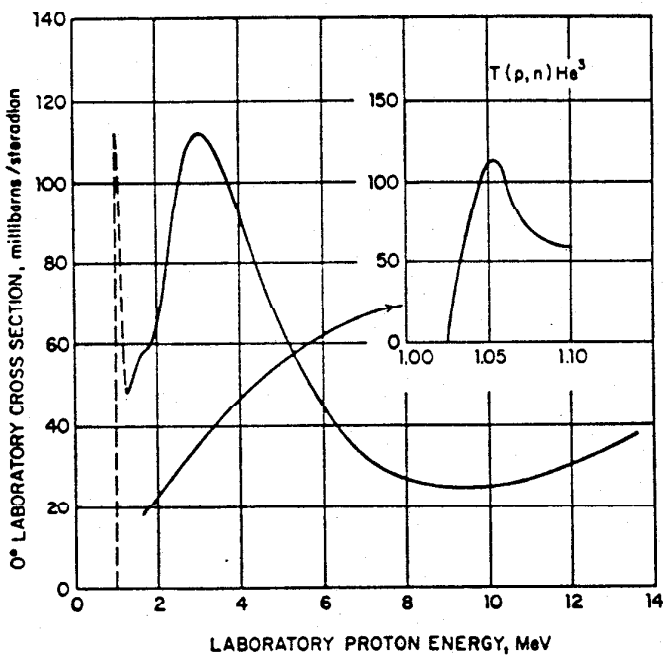


FIG. 8f-12. The laboratory 0-deg production cross section for the $\text{T}(\text{p},\text{n})$ neutron source reaction.

acter of the beam would be the many-body breakup of the triton. The threshold for this reaction is at 8.34 MeV, but no breakup has been observed up to a proton energy of 13 MeV (0 deg breakup production cross section <5 millibarns/steradian). Measured differential cross section for the $\text{T}(\text{p},\text{n})$ reaction can be transformed to the center-of-mass system and fitted by a sum of Legendre polynomials; i.e., $\sigma(\theta_{\text{cm}}) =$

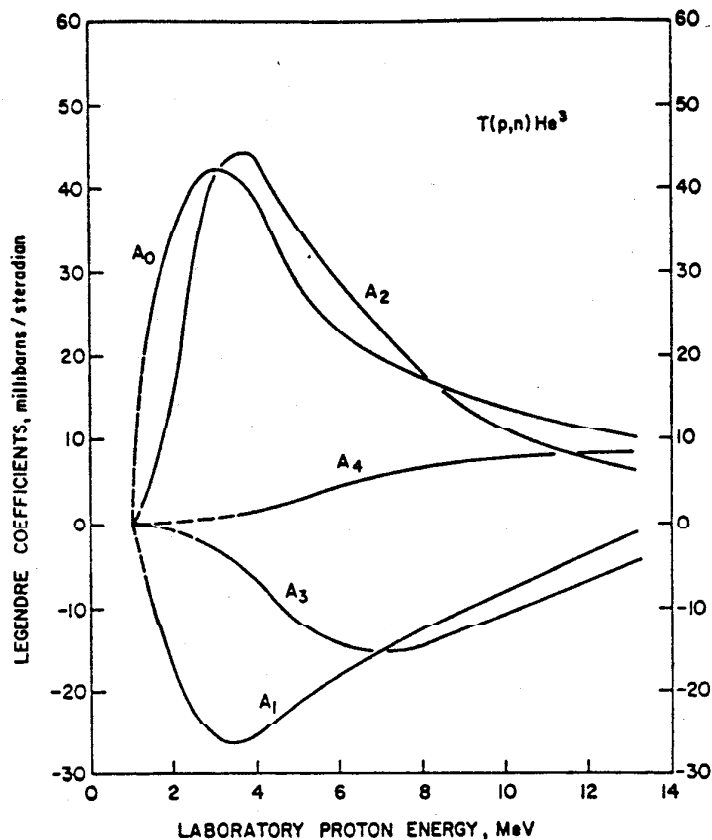


FIG. 8f-13. Variation of the Legendre-sum fitting coefficients for the $T(p,n)$ reaction with proton energy. The fitting is done for data in the center-of-mass system. The total integrated production cross section for the reaction is equal to $4\pi A \times 10^{-2}$.

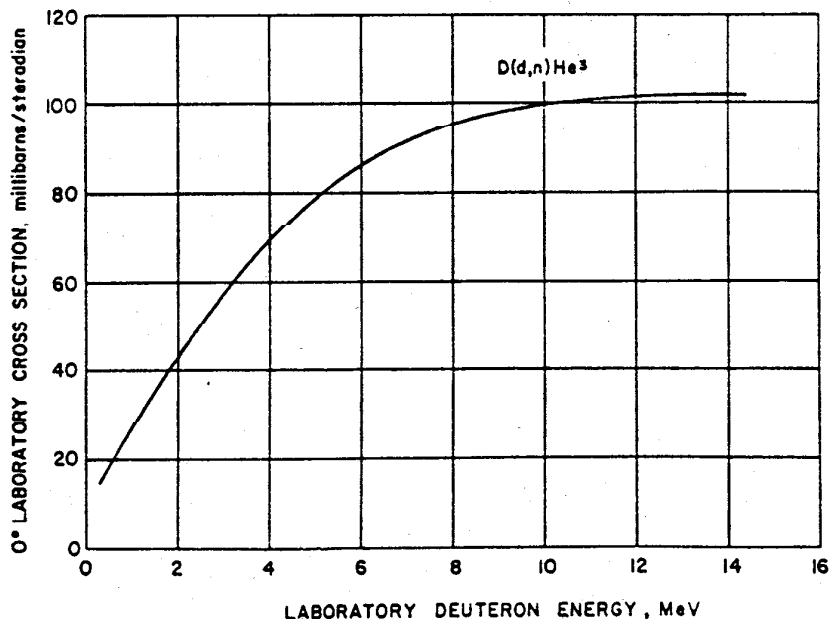


FIG. 8f-14. The laboratory 0-deg production cross section for the $D(d,n)$ neutron source reaction.

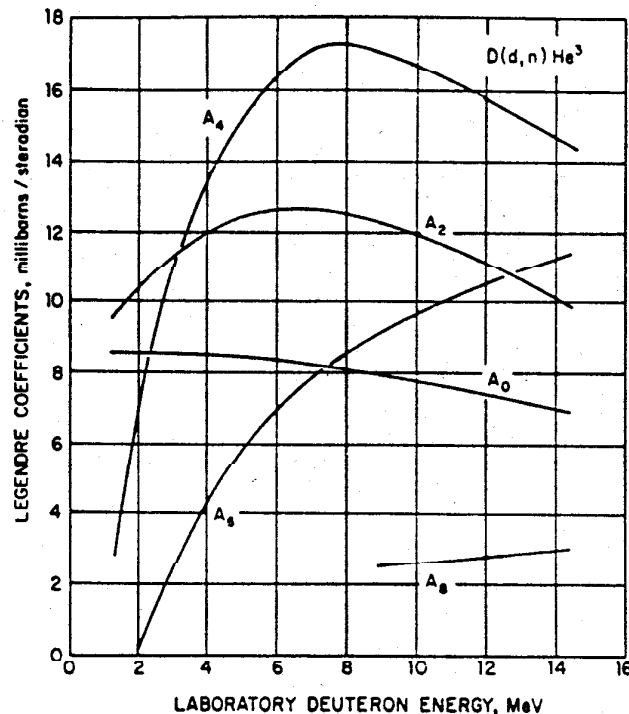


FIG. 8f-15. Variation of the Legendre-sum fitting coefficients for the $D(d,n)$ reaction with deuteron energy. The fitting is done for data in the center-of-mass system. The total integrated production cross section for the reaction is equal to $4\pi \cdot 4 \cdot 10^2$.

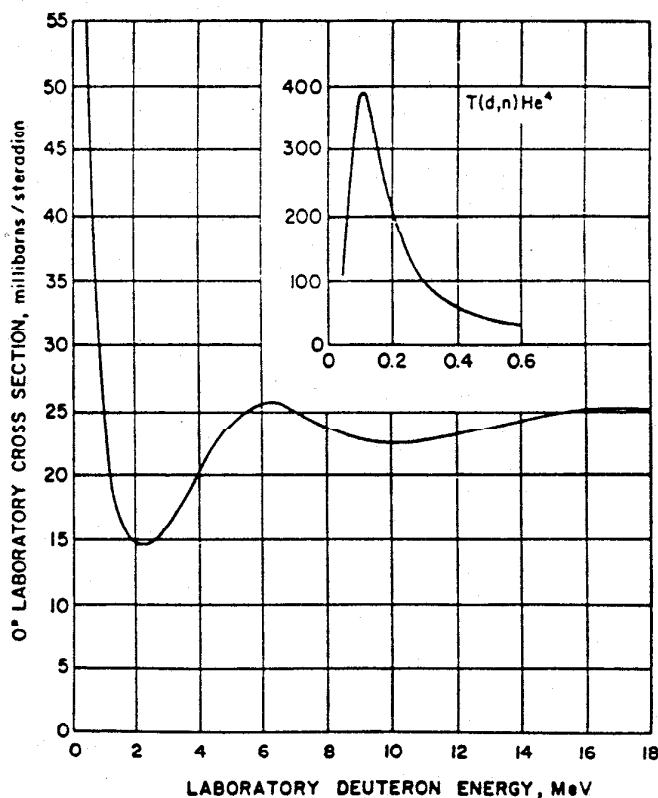


FIG. 8f-16. The laboratory 0-deg production cross section for the $T(d,n)$ neutron source reaction.

$\sum A_n P_n(\cos \theta_{cm})$. A plot of the variation of the fitting coefficients with energy allows construction of angular distribution curves at any energy through the range shown. For this reaction, Fig. 8f-13 shows such a plot. One can also see the shape of the total integrated production cross section (as well as obtain values) from the variation of the A_0 coefficient, since this cross section is equal to $4\pi A_0^2$.

The $D(d,n)\text{He}^3$ reaction has a Q value of +3.268 MeV and is thus exoergic. As can be seen from Fig. 8f-10, the neutron energy at 0 deg for cascade-generator deuteron energies is ≈ 3 MeV. The laboratory 0 deg production cross section is shown in Fig.

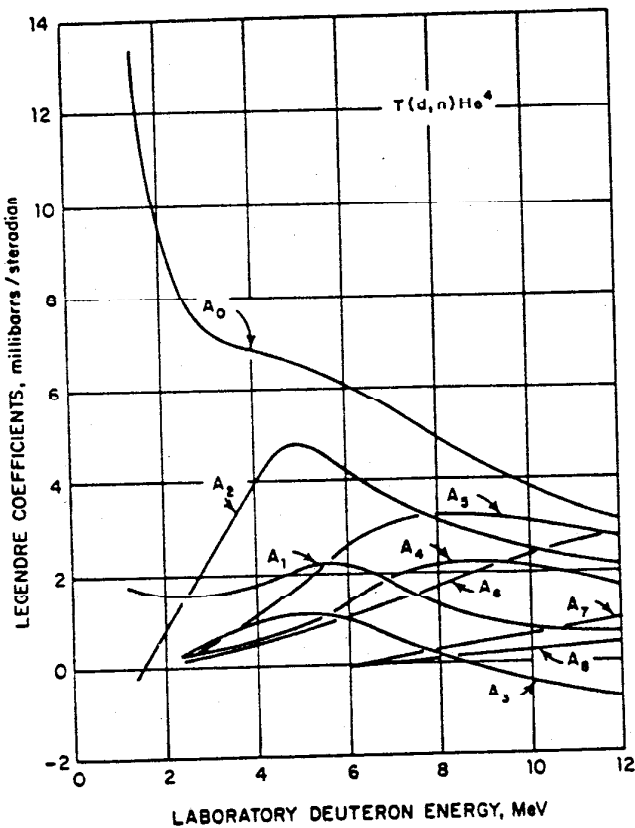


FIG. 8f-17. Variation of the Legendre-sum fitting coefficients for the $T(d,n)$ reaction with deuteron energy. The fitting is done for data in the center-of-mass system. The total integrated production cross section for the reaction is equal to $4\pi A_0^2$.

8f-14. The cross section approaches zero smoothly with decreasing deuteron energy, and so fluxes at cascade generator energies are not as copious as with the $T(d,n)$ reaction (see below). The threshold for deuteron breaking is at 4.45 MeV, and this reaction cross section increases rapidly and is a significant contaminant for deuteron energies above about 6 MeV. Usually energy-discriminating devices are adequate to separate breakup neutrons from the primary group. As described above, angular distributions and the total production cross section can be obtained, using the Legendre fitting coefficients shown in Fig. 8f-15.

The $T(d,n)\text{He}^4$ reaction has a Q value of +17.588 MeV and is thus exoergic. As can be seen from Fig. 8f-10, neutron energies at 0 deg near zero deuteron energy begin at near 15 MeV. The laboratory 0 deg production cross section is shown in Fig. 8f-16. The large production cross section at a deuteron energy of 110 keV, due to a resonance

in He^3 , makes this reaction a copious source of high-energy neutrons for deuteron energies available with cascade generators. As can be seen from the top insert in Fig. 8f-10, the energy varies less rapidly at 90 than at 0 deg, and many experiments have been done at this angle. The threshold for deuteron breakup is 3.71 MeV, but the large energy gap between the breakup and primary groups makes energy discrimination quite easy. As described above, angular distributions and the total production cross section can be obtained using the Legendre fitting coefficients shown in Fig. 8f-17.

8f-10. Cross-section Compilation Bibliography. The Sigma Center (now part of the National Neutron Cross Section Center) at Brookhaven National Laboratory has produced over the years compilations of measured neutron cross-section data and parametric information derived from these measurements. Below are listed still current volumes from this work.

1. Hughes, Donald J., and Robert B. Schwartz: "Neutron Cross Sections," BNL 325, 2d ed., July, 1958.
2. Hughes, D. J., B. A. Magurno, and M. K. Brussel: "Neutron Cross Sections," BNL 325, 2d ed., supplement 1, Jan. 1, 1960.
3. Stehn, John R., et al., "Neutron Cross Sections," BNL 325, 2d ed., supplement 2, vol. 1, [Z = 1-20], May, 1964.
4. Goldberg, Murray D., et al., "Neutron Cross Sections," BNL 325, 2d ed., supplement 2, vol. IIA [Z = 21-40], February, 1966; *ibid.*, vol. IIB [Z = 41-60], May, 1966; *ibid.*, vol. IIC [Z = 61-87], August, 1966.
5. Stehn, John R., et al., "Neutron Cross Sections," BNL 325, 2d ed., supplement 2., vol. III [Z = 88-98], February, 1965.
6. Garber, Donald L., et al., "Angular Distributions in Neutron-induced Reactions," BNL 400, 3d ed., vol. I [Z = 1-20] and vol. II [Z = 21-94], 1970.

The world's experimental neutron cross-section data are stored at Brookhaven on magnetic tape and are available to those who request them.